00000337
CTD/ADM-DMC

ORNL/TM-5883

Actinide Partitioning and Transmutation Program Progress Report for Period October 1, 1976 to March 31, 1977

J. O. Blomeke
D. W. Tedder

OAK RIDGE NATIONAL LABORATORY
OPERATED BY UNION CARBIDE CORPORATION FOR THE ENERGY RESEARCH AND DEVELOPMENT ADMINISTRATION

ORNL/TM-5888

Contract No. W-7405-eng-26

CHEMICAL TECHNOLOGY DIVISION

ACTINIDE PARTITIONING AND TRANSMUTATION PROGRAM

PROGRESS REPORT FOR PERIOD OCTOBER 1, 1976 TO MARCH 31, 1977

Compiled by:

J. O. Blomeke

D. W. Tedder

Date Published: June 1977

NOTICE This document contains information of a preliminary nature. It is subject to revision or correction and therefore does not represent a final report.

Oak Ridge National Laboratory
Oak Ridge, Tennessee 37830
operated by
UNION CARBIDE CORPORATION
for the

ENERGY RESEARCH AND DEVELOPMENT ADMINISTRATION

CONTENTS

Foreword v

Summary vii

1. Purex Process Modifications 1

2. Actinide Recovery from Solids 11

3. Americium-Curium Recovery with OPIX, TALSPEAK, and CEC. 17

4. Americium-Curium Recovery Using Bidentate Extractants 18

5. Americium-Curium Recovery Using Inorganic Ion Exchange Media. . . . 22

6. Recovery Alternatives Applicable to Waste Streams 27

7. Actinide Recovery from Combustible Waste. 51

8. Actinide Recovery and Recycle Preparation for Waste Streams 58

9. Radiation Effects 67

10. Fuel and Target Fabrication Studies 75

11. LMFBR Transmutation Studies 76

12. Thermal Reactor Transmutation Studies 78

13. Fuel Cycle Impact Studies 79

14. Risk/Benefit Analysis of Concept. 79

15. Detailed Economic Analysis of Fabrication and Reprocessing Plants in a Partitioning-Transmutation Fuel Cycle 79

16. Partitioning-Transmutation Analysis, Coordination, and Evaluation 80

FOREWORD

This is the first in a series of progress reports to be issued on the Actinide Partitioning and Transmutation Program, which is a multisite effort coordinated at the Oak Ridge National Laboratory. Its overall objective is to evaluate the feasibility and incentives for partitioning (separating) the long-lived biologically significant isotopes from fuel cycle wastes and transmuting (burning) them to shorter-lived or stable isotopes in power reactors.

During FY 1977 and 1978, the principal emphasis of the program will be on the experimental evaluation of partitioning actinides, followed by their recovery in forms suitable for fabrication into transmutation targets. Detailed computer analyses will be undertaken to determine the effects on reactor and fuel cycle operations of recycling the partitioned actinides and to further verify the feasibility of transmutation itself. In FY 1979 the major effort will be directed toward a detailed assessment of the costs, risks, and benefits associated with this concept. The program is expected to produce: (1) realistic reprocessing and refabrication flowsheets which have been at least partly verified by experimental work, (2) several realistic transmutation schemes based on sophisticated reactor physics calculations, (3) an evaluation of partitioning and transmutation impacts on all phases of the nuclear fuel cycle, (4) a meaningful risk-cost-benefit analysis, and (5) a program plan for future development and demonstration requirements for eventual implementation in

commercial operations. This analysis should constitute a reasonably firm technical basis for determining whether partitioning-transmutation represents a viable waste management alternative for managing long-lived waste nuclides that are generated by a nuclear power economy.

The program consists of 16 major tasks. This report summarizes the work done on each of these during the initial six-month period.

SUMMARY

Experimental work on the 16 tasks comprising the Actinide Partitioning and Transmutation Program was initiated at the various sites. This work included the development of conceptual material balance flowsheets which define integrated waste systems supporting an LWR fuel reprocessing plant and a mixed (U-Pu) oxide fuel refabrication plant. In addition, waste subsystems were defined for experimental evaluation. Computer analysis of partitioning-transmutation, utilizing an LMFBR for transmutation, was completed for both constant and variable waste actinide generation rates.

1. PUREX PROCESS MODIFICATIONS

W. D. Bond, F. A. Kappelmann, S. Katz, and F. M. Scheitlin (Oak Ridge National Laboratory)

This task focuses on modifications to the Purex process which should result in higher recoveries of uranium, neptunium, and plutonium. Modifications to the process operations are considered, as well as alternatives in cleanup systems which result in smaller waste volumes and actinide losses.

The Purex process employs tributyl phosphate (TBP), usually at a concentration of 30 vol %, in a hydrocarbon diluent (*n*-dodecane) to extract uranium and plutonium from fuel dissolver solutions. The degree of recovery is dictated both by the extent of extractability of these actinides from an aqueous solution salted by nitric acid and by the effectiveness of stripping the actinides from the extractant. Nominally, each of the extractable actinides undergoes at least two cycles (extraction and stripping) of solvent extraction to achieve the necessary decontamination from fission products and separation from each other. Any actinides not extracted from the solution of dissolved fuel remain with the high-level aqueous waste, whereas any actinides not stripped from the organic phase report to the wastes resulting from the regeneration and recycle of the extractant. In existing Purex plants, the extractant is purified for recycle by scrubbing it with an aqueous sodium carbonate solution, which removes most of the principal solvent degradation products as well as the actinides and fission products. Thus, the sodium carbonate solution becomes a transuranic waste stream, requiring further treatment in waste management. The actinide values remaining in nitric acid streams

from the second and third Purex cycles (purification cycles) appear to be amenable to recycle if appropriate oxidation and reduction methods are used to separate the actinides from each other.

Laboratory work carried out during this report period includes the following studies:

(1) Extraction and stripping of uranium using simulated, nonradioactive fuel dissolver and high-level waste solutions as feeds.

(2) Removal of actinides from simulated sodium carbonate solvent cleanup waste.

1.1 Extraction and Stripping of Uranium and Plutonium

Experiments are being carried out on the Purex process relative to the countercurrent extraction and stripping of actinides using both continuous mixer-settlers and batch equipment. The purpose of these experiments is to determine the effects on actinide losses by either including additional stages of extraction and stripping or using an additional Purex cycle to remove actinides from the high-level waste stream. The effects of the increased extraction of the zirconium and ruthenium fission products are also being evaluated. It is not known whether the increased radiation damage caused by the additional extraction stages (or cycles) will result in interfacial precipitates and cruds. Zirconium compounds formed with degradation products are reported to be of limited solubility both in the organic and aqueous phases and have been observed to impair operability when high-burnup fuels are processed.

1.1.1 Studies using mixer-settlers

Four experimental runs have been made using continuous, countercurrent mixer-settler equipment. Results obtained from two of the runs which involved extraction and stripping of uranium showed that >99.9% of the uranium was recovered. The uranium losses to the aqueous raffinate using 8 extraction stages and 8 scrubbing stages was <0.01%, whereas losses to the stripped organic was about 0.02% using 16 stripping stages. Two runs were also made to estimate the extent of zirconium extraction in a second cycle of Purex for removing actinides from high-level waste. Analytical results from the zirconium experiments are not yet available.

Equipment. The equipment used in this study (see Fig. 1.1) consists of two mixer-settler banks: one bank for extraction-scrubbing, and the other for stripping. Each bank is comprised of 16 stages. A close-up photograph of some of the stages of the extraction-scrubbing bank is shown in Fig. 1.2.

Results. Work performed to date has been carried out using simulated feed solutions (i.e., using nonradioactive isotopes of the fission products in concentrations corresponding to PWR-U fuel irradiated to 33,000 MWD/tonne*). In our first two runs, we determined the recovery of uranium from nitric acid solution alone (Run R-1) and from a nitric acid solution containing cold fission products (Run R-2). In the extraction-scrubbing bank, 8 stages of extraction and 8 stages of scrubbing were employed using 30% TBP--dodecane. The feed solution in each case was 1.3 M in

---

*In this report, "tonne" is used to mean metric ton.

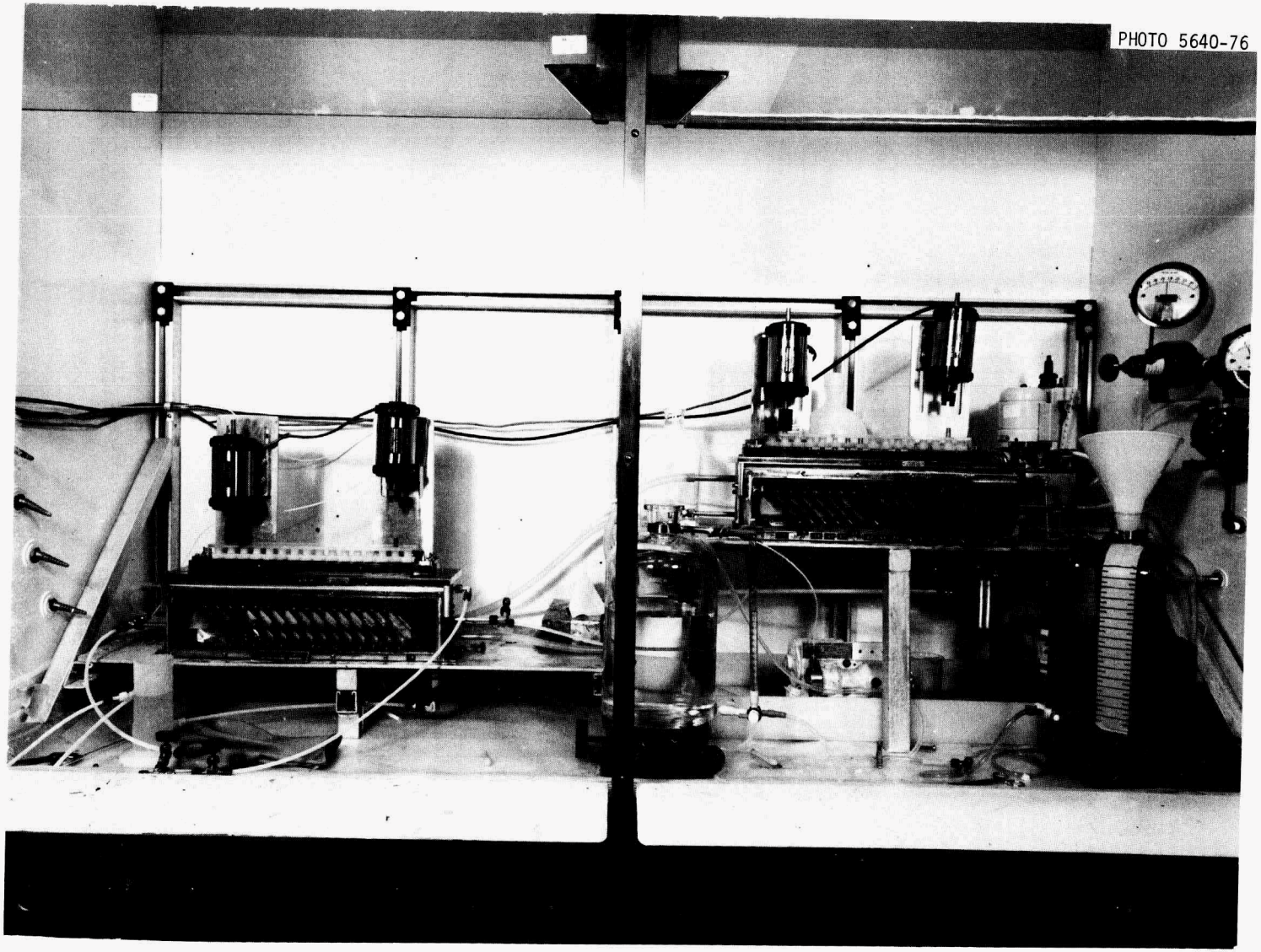

Fig. 1.1. Overall view of mixer-settler equipment.

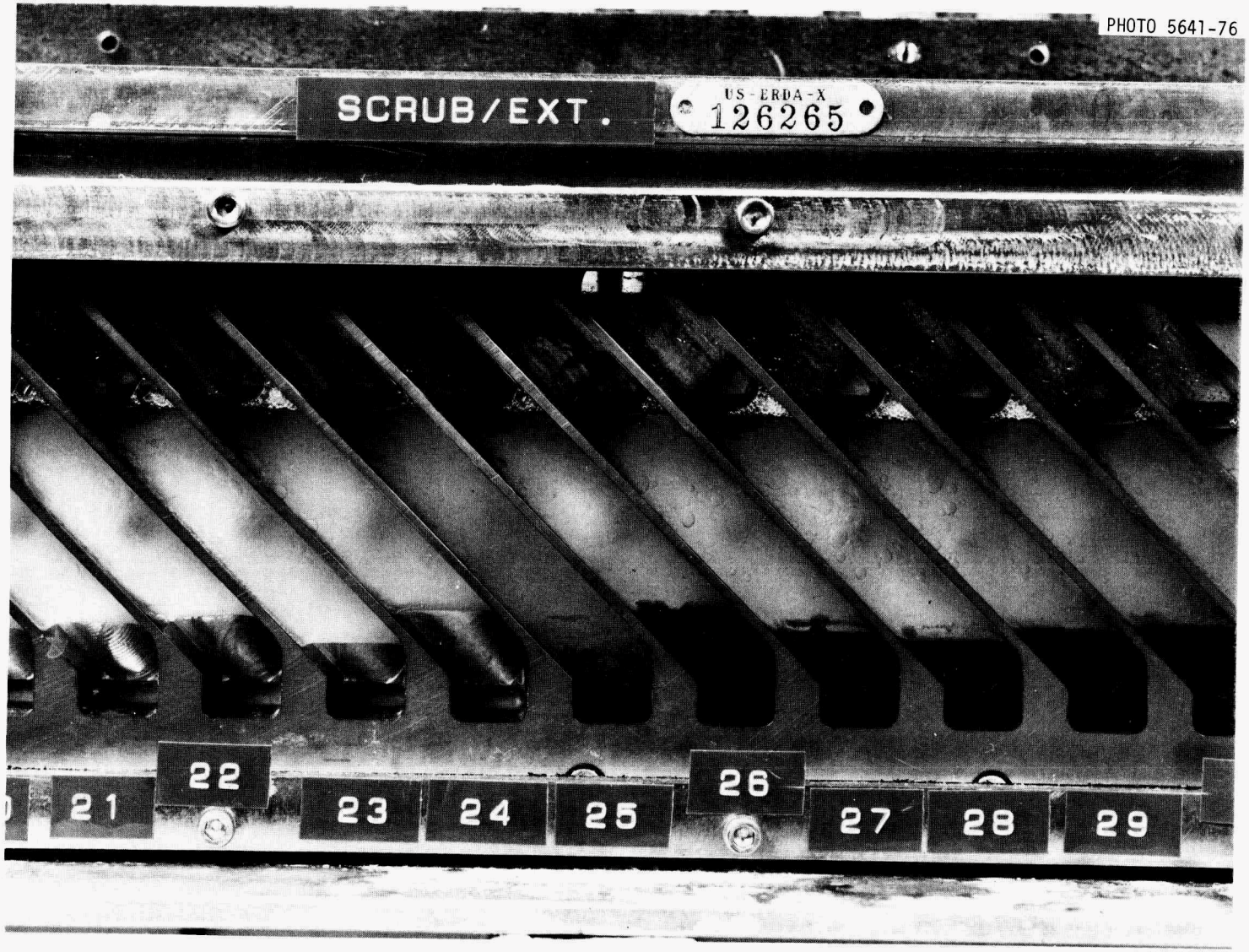

Fig. 1.2. Close-up of extraction and scrubbing stages during run R-2. Feed stage = 25.

uranium and 2.5 M in HNO_3, and the concentration of nitric acid used for scrubbing was 3.0 M. The flow rates for the feed, scrub, and extractant solutions were 0.5, 0.2, and 1.75 liters/hr respectively. The exiting extractant stream was fed to the stripping bank and contacted with 0.3 M HNO_3 solution flowing at 4.0 liters/hr. The experiments were carried out over a 16-hr period to permit attainment of steady state. At the end of the run, equilibrium distribution measurements were made in order to determine the efficiency of the mixer-settler banks. The stripping solution was introduced at two points in order to avoid phase disengagement difficulties with the stripping bank. It was metered to stage 1 at 0.5 liter/hr and to stage 5 at 3.5 liters/hr. The uranium-laden solvent from the extraction-scrubbing bank, flowing at 1.75 liters/hr, entered stage 16 of the stripping bank. The difficulty with phase disengagement, which was caused by inadequate pumps, has been resolved by the installation of new pumps. This should eliminate the need to divide the aqueous stripping solution in future experiments.

Material balance data on uranium for the two runs are shown in Table 1.1. The uranium content of the aqueous product was computed from the uranium losses to the aqueous raffinate and the stripped organic. Most of the loss is due to incomplete stripping of the organic phase. In a conventional Purex plant, the unstripped uranium would report to the solvent recycle waste.

Table 1.1. Material balance of uranium in the mixer-settler tests

Run number	Uranium content (%)		
	Aqueous raffinate	Stripped organic	Aqueous product
R-1	0.0002	0.006	99.99
R-2	<0.01	0.02	>99.97

Measurements of the equilibrium distribution coefficients for each stage of the extraction-scrubbing and stripping banks indicated that the stage efficiency for each bank was about 70%. These measurements were in general agreement with calculations made by using the SEPHIS computer code.[1]

1.1.2 Batch countercurrent extraction studies

Extraction experiments are being carried out to generate equilibrium distribution coefficient data for the extraction of uranium, plutonium, and key fission products into TBP. The data from these experiments will increase our confidence in calculations made using the SEPHIS code. The work performed to date has consisted of experimental studies on the extraction of uranium, zirconium, ruthenium, and molybdenum from both HNO_3 and simulated LWR fuel dissolver solutions. Installation of equipment in a glove box for plutonium extraction studies is nearly complete.

Four extraction stages and three scrubbing stages were employed in countercurrent extraction experiments; seven stripping stages were used in stripping experiments. Five extraction experiments and two stripping experiments have been carried out to determine the distribution of uranium and HNO_3 between the aqueous and organic phases. The experimental results

obtained do not agree with SEPHIS calculations, and the discrepancy has been traced to faulty analysis of HNO_3. The results shown for one of the stripping experiments (Table 1.2) are typical of those obtained thus far. Work on obtaining reliable analyses of HNO_3 is currently in progress.

Several experiments have been conducted to determine the distribution of zirconium, ruthenium, and molybdenum in the extraction and scrubbing stages. In the early runs we used spark-source mass spectroscopy to detect the elemental distribution; however, this approach was unsuccessful because of the low concentrations of the elements in the organic phase, particularly in the scrubbing stages.

Radioactive tracers are currently being used to determine the distribution of the fission products. Two zirconium extraction runs have been made in which fission products were present in concentrations expected in the high-activity solvent extraction feed. Results are shown in Table 1.3. The extraction behavior generally agreed with that expected from literature data.

1.1.3 Removal of actinides from sodium carbonate scrubber solutions

Initial tests of a method based on nitric acid treatment of simulated solvent cleanup waste showed promise for removing plutonium from these wastes by anion exchange or by TBP extraction. The nitric acid treatment consisted of adding excess HNO_3 to the simulated Na_2CO_3 waste solution and refluxing the solution to promote dealkylation and hydrolysis of monobutyl (MBP) and dibutyl phosphoric (DBP) acid. These tests were conducted with tracer-level plutonium in a 0.2 $\underline{M}$ Na_2CO_3 solution to which a mixture of MBP and DBP (55%-45%) had been added to make their combined

Table 1.2. Comparison of experimental distribution of uranium and HNO_3 with values calculated by the SEPHIS code

Aqueous strip: 0.126 M HNO_3; volume entering stage 7 = 33 ml
Organic feed: 28.8% TBP, 87.8 g U/liter--0.066 M HNO_3; volume entering stage 1 = 30 ml

Stage number	Organic phase				Aqueous phase			
	HNO_3 (M)		Uranium (g/liter)		HNO_3 (M)		Uranium (g/liter)	
	Exptl.	SEPHIS	Exptl.	SEPHIS	Exptl.	SEPHIS	Exptl.	SEPHIS
1	0.14	0.001	74.8	72.8	0.40	0.127	66.9	72.4
2	0.16	0.009	67.0	60.8	0.50	0.126	58.4	58.7
3	0.17	0.01	59.5	50.7	0.32	0.126	49.2	48.0
4	0.19	0.01	49.8	40.9	0.26	0.125	39.8	39.9
5	0.21	0.016	38.3	30.5	0.24	0.124	31.6	30.4
6	0.14	0.016	28.3	18.6	0.22	0.126	23.4	21.1
7	0.02	0.009	13.8	6.6	0.19	0.174	13.5	10.5

concentrations 0.07 M. After the nitric acid treatment, about 95% of the plutonium could be absorbed on an anion exchange bed from 8 M HNO_3. Reflux tests showed that 14 M HNO_3 was more efficient in destroying the MBP and DBP than were 2, 8, and 11 M HNO_3; with this treatment, about 90% of the MBP and DBP were converted to free phosphate ion after 12 hr. The organic compounds formed by oxidation of the butyl groups have not been identified.

Table 1.3. Countercurrent extraction of zirconium from simulated fission products

Aqueous feed: Simulated fission products in 2 M HNO_3; volume entering stage 4 = 15 ml
Organic: 30% TBP; volume entering stage 1 = 30 ml
Scrub: 2 M HNO_3; volume entering stage 7 = 15 ml

Stage number	Distribution coefficient (O/A)	
	2-min contact	10-min contact
1	0.030	0.039
2	0.040	0.046
3	0.040	0.045
4	0.035	0.034
5	0.083	0.076
6	0.073	0.054
7	0.14	0.093

1.2 Reference for Section 1

1. S. B. Watson and R. H. Rainey, Modifications of the SEPHIS Code for Calculating the Purex Solvent Extraction System, ORNL/TM-5123 (December 1975).

2. ACTINIDE RECOVERY FROM SOLIDS

E. L. Lewis and D. F. Luthy (Mound Laboratory)

The objective of this task is to measure the ability to decontaminate solids using reagents which are compatible with the reprocessing and refabrication flowsheets. The initial studies focus on the ability to decontaminate HEPA filters.

2.1 Experimental Work

Efforts during this report period were directed toward determining the dissolution parameters of plutonium in nitric acid. The parameters determined include the optimum acid concentration and the optimum dissolution temperature.

Contaminated HEPA filter media were prepared by mixing PuO_2* powder with shredded filter media. The resulting mixture contained ∿0.2 Ci (11 mg) of ^{238}Pu per cubic centimeter of prepared media. Small samples of this mixture (∿3.0 g) were put into beakers containing 250 ml of HNO_3 of the desired concentration. The beakers and contents were then heated to the desired temperatures. Samples were taken every 4 to 8 hr and the ^{238}Pu concentration of the acid solution determined. The beaker contents were stirred every hour, with one exception in which constant magnetic stirring was used. The solution volume and concentration were adjusted when necessary by adding nitric acid to the beaker to replace evaporated acid.

---

*This powder, which has an average particle size of ∿20 μ, is a mixture of plutonium oxides (80% ^{238}Pu, 16% ^{239}Pu, 2.5% ^{240}Pu, 0.8% ^{241}Pu, 0.2% ^{242}Pu) plus very small amounts of other actinides.

Table 2.1 shows results from dissolution tests using nitric acid of various concentrations (6, 8, 10, 12, and 15.7 M). It should be noted that the optimum acid concentration was 8 M, and the optimum temperature at this concentration was ∿120°C (boiling). The maximum amount of PuO_2 dissolved was 9.03% after 18.5 hr of heating (see acid test No. 6-3).

The data in Fig. 2.1 show how the dissolution rates vary with temperature. This plot, which is for 6 M HNO_3, is generally similar to the plots for 8, 10, 12, and 15.7 M with one exception. That is, the maximum dissolution rate for 10 M HNO_3 was not at the boiling temperature, but at 95°C. Therefore, the tests with 10 M HNO_3 will be rerun to investigate this phenomenon.

The data in Fig. 2.2 illustrate the effect of stirring on the dissolution rates. As can be seen, the dissolution rates are essentially identical; the small difference could be due to experimental error. One explanation for the identical rates is that both solutions are actually undergoing constant mixing, one of them due to convection currents caused by constant external heating and the other as a result of mechanical stirring.

The effect of dissolution of asbestos and fiberglass in the filter media is not presently known. Isotherms will be run to determine the effect, if any, the media has on the solubility and dissolution rates of the PuO_2.

2.2 Conclusions

Dissolution tests were conducted with 6, 8, 10, 12, and 15.7 M HNO_3 on filter media contaminated with PuO_2. The optimum acid concentration and temperature were 8 M and boiling (∿120°C) respectively. The amount of PuO_2 dissolved after 18.5 hr was, however, only 9.0 wt %. This work substantiates data collected in recovery operations at Mound Laboratory,

Table 2.1. PuO_2 dissolution tests with shredded HEPA filter media

Acid test number	Acid conc. (M)	Acid temperature (°C)	Time (hr)	PuO_2[a] dissolved (mg)	PuO_2[a] dissolved (wt %)
1-1	6	80	4	1.40	0.88
1-2	6	80	8	1.89	1.18
1-3	6	80	13.5	2.73	1.71
2-1	6	90	4	1.62	1.07
2-2	6	90	8	2.22	1.47
2-3	6	90	13.5	3.28	2.17
3-1	6	Boiling	2.5	2.00	1.31
3-2	6	Boiling	5.5	2.82	1.84
3-4	6	Boiling	10.5	3.80	2.48
4-1	8	85	4	2.40	1.62
4-2	8	85	8	2.75	1.86
4-3	8	85	13	5.50	3.72
5-1	8	95	4	2.75	1.86
5-3	8	95	8	3.50	2.36
5-4	8	95	13	6.12	4.14
6-1	8	Boiling	6	5.40	3.75
6-2	8	Boiling	12.5	5.80	4.03
6-3	8	Boiling	18.5	13.00	9.03
7-1	10	85	6.5	2.75	1.88
7-2	10	85	11.5	4.00	2.73
7-3	10	85	16.25	4.14	2.82
8-1	10	95	6.5	4.50	3.20
8-2	10	95	11.5	5.85	4.15
8-3	10	95	16.25	6.90	4.90
9-1	10	Boiling	6.5	3.75	2.39
9-2	10	Boiling	11.5	4.73	3.01
9-3	10	Boiling	16.25	6.35	4.04
10-1	12	85	6.5	2.80	1.68
10-2	12	85	11.5	4.00	2.40
10-3	12	85	16.25	5.13	3.08
11-1	12	95	6.5	4.00	2.39
11-2	12	95	11.5	5.40	3.22
11-3	12	95	16.25	5.63	3.36
13-1	12	Boiling	4.5	5.64	3.78
13-2	12	Boiling	11.25	8.80	5.90
13-3	12	Boiling	18	8.48	5.68
14-1[b]	10	95	4.5	3.70	2.68
14-2[b]	10	95	9.25	4.90	3.55
14-3[b]	10	95	16.25	5.95	4.31
15-1	15.7	85	5	4.41	3.35
15-2	15.7	85	13	4.94	3.76
15-3	15.7	85	16.5	4.83	3.68
16-1	15.7	95	5.5	4.41	3.14
16-2	15.7	95	13	3.83	2.72
16-3	15.7	95	16.5	5.52	3.93
17-1	15.7	Boiling	6.25	6.67	4.70
17-2	15.7	Boiling	3	6.60	4.65
17-3	15.7	Boiling	16.75	6.67	4.70

[a]Expressed as plutonium metal.

[b]Beaker contents were stirred continuously by magnetic stirring bar.

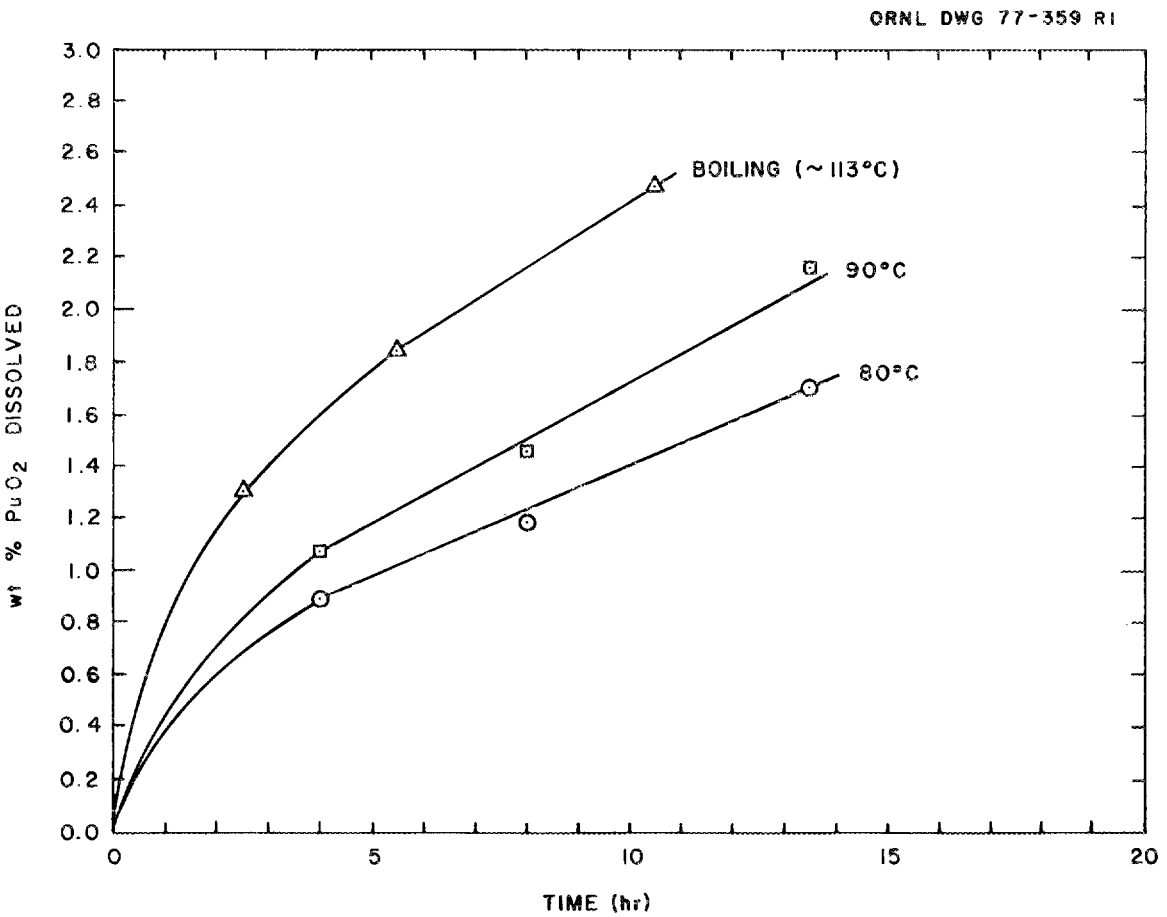

Fig. 2.1. Comparison of the dissolution rates of PuO_2 in 6 M HNO_3 at selected temperatures.

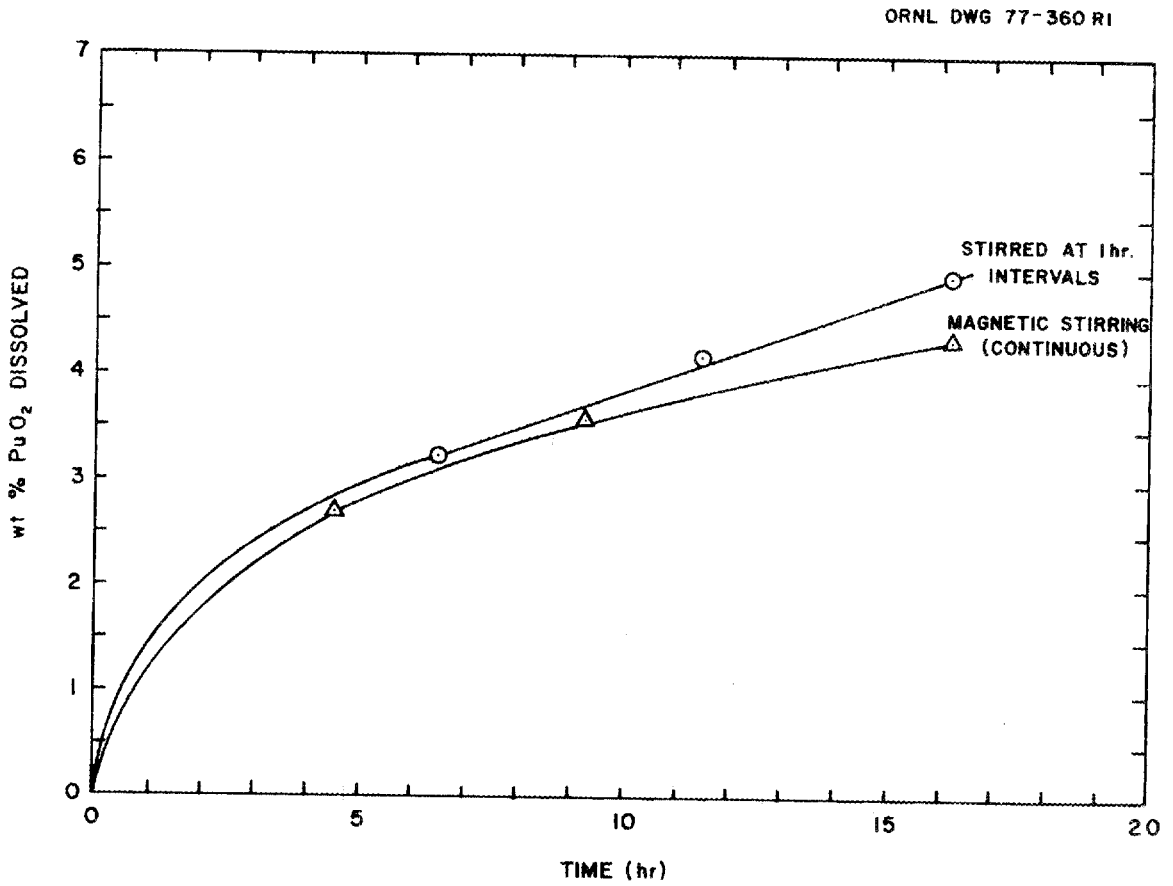

Fig. 2.2. Comparison of effect of stirring on dissolution rate of PuO_2 in 10 M HNO_3 at 95°C.

indicating that nitric acid alone is not an effective leachant. However, such data provide basic information on the effects of the filter media on the equilibrium reaction, showing that stirring of the leach solutions has no effect on the dissolution rate. During the next quarter, other leachants will be investigated. These will include HNO_3 with a dilute concentration of HF; HNO_3 in combination with small percentages of H_2SO_4; HNO_3 with ceric salts[1]; and combinations of HNO_3, HF, and H_2SO_4.[2] Also, the use of electrolytic oxidation[3] to dissolve plutonium in HNO_3-HF solutions, as well as ultrasonic agitation of leach reagents,[4] might be investigated to determine whether such approaches have merit for this application.

2.3 References for Section 2

1. G. L. Silver, Dissolution Processes, MLM-2372, p. 3 (October 1976).
2. C. H. H. Chong, T. W. Crockett, and J. W. Doty, Jr., J. Inorg. Nucl. Chem. 31, 81 (1969).
3. G. L. Silver, Dissolution Processes, MLM-2372, p. 7 (October 1976).
4. Plutonium Processing at the Los Alamos Scientific Laboratory, LA-3542 (April 1969).

3. AMERICIUM-CURIUM RECOVERY WITH OPIX, TALSPEAK, AND CEC

W. D. Bond and C. W. Forsberg (Oak Ridge National Laboratory)

This work examines the use of oxalate precipitation and cation exchange (OPIX process) to remove the lanthanides and transplutonium actinides from the high-level liquid waste produced by the Purex solvent extraction process. TALSPEAK solvent extraction and cation exchange chromatography (CEC) are studied as methods of separating the lanthanides and trivalent actinides.

The principal activities during this report period were the design of a laboratory-scale experiment and initiation of the procurement of the necessary equipment to evaluate the feasibility of carrying out the OPIX process continuously. The main purpose of the experiment is to determine whether continuous settling and decantation is a viable approach in collecting the oxalate precipitate. Variables that will be studied include: (1) precipitation and crystallization rate, (2) settling time of the crystals, (3) equilibrium acidity and oxalic acid concentration, and (4) temperature. The effects of these variables will be correlated with the relative recoveries obtained in the precipitation and ion exchange steps. Initial studies will be limited to definitive investigations involving the use of a nitric acid solution of lanthanide elements as the feed solution. In subsequent experiments, we expect to determine the effects of variables on the decontamination factors achieved in the oxalate precipitation step. Previous studies using batch precipitations have shown that a few percent of the zirconium is precipitated along with the trivalent actinides and lanthanides. Zirconium has an adverse effect in the Talspeak process.

4. AMERICIUM-CURIUM RECOVERY USING BIDENTATE EXTRACTANTS

L. D. McIsaac (Allied Chemical Corporation-Idaho Chemical Programs)

The objective of this task is to study the usefulness of neutral bidentate extractants in recovering the transplutonium actinides from the HLLW. One phase of this study involves the development of flowsheets which describe the extraction of the actinides and lanthanides, their decontamination from other fission products, the stripping of the extractant, and the cleanup of the used solvent for recycle.

The bidentate extractants proposed for this study are presently obtainable only in a crude form which is not satisfactory for use. At this time, we are using a "small" high-vacuum distillation system to obtain ∿86% pure dihexyl-N,N-diethylcarbamylmethylenephosphonate (DHDECMP) after two distillations. This is a very slow process, and we will not be able to come close to obtaining the ultrapure DHDECMP needed until a preparative high-pressure liquid chromatograph system is installed. We will, however, be able to use this 86% DHDECMP for preliminary studies.

Radioactive nuclides to be used for extraction studies have been ordered. Some are in our possession now, and a few will be prepared locally when we have sufficient amounts of extractant to begin. We are investigating methods for selectively stripping actinides from the extractant and subsequent cleanup of the solvent for recycling purposes.

4.1 Preparation of Synthetic Waste Solution

Initial studies will be conducted using synthetic waste solution prepared by mixing nitric acid solutions of nitrate salts of nonradioactive isotopes of fission product elements. The quantities are based

on those that were calculated by the ORIGEN code for typical PWR-U fuel irradiated to 33,000 MWd/tonne. The fission-product content is based on reprocessing after a postirradiation decay time of 160 days and storage of wastes in liquid form for five years after reprocessing. The volume, acid concentration, and fission-product content values correspond to approximately those expected, after the codecontamination step, in the HAW column (5569 liters, 2.9 M HNO_3) before exhaustive extraction with 30% TBP. This step was chosen because this is a possible location for our bidentate extraction process. For our early experiments, 2 liters of solution would be sufficient; however, a solution that was prepared by dissolving all the water-solubles and adding the dissolved material to a solution of the 2.9 M HNO_3-solubles plus the elements dissolved in concentrated HNO_3 proved unsatisfactory. With time, a precipitate appeared. This precipitate, which has been submitted for analysis, is assumed to be a zirconium-molybdenum complex; however, its actual composition cannot be reported until the analytical results become available. We have found that $ZrO(NO_3)_2 \cdot 4H_2O$ will dissolve in 2.9 M HNO_3, but does precipitate with time. Tin and antimony are not stable with regard to precipitation. We encountered considerable difficulty in trying to dissolve dry $Pd(NO_3)_2$ in water and in 2.9 M HNO_3, but palladium sponge dissolved in concentrated nitric acid and remained in solution. Filtration of the waste solution immediately after preparation showed that some palladium had precipitated.

We will continue to investigate other methods of solution preparation which will give a stable product. However, at present, it appears that our procedure will be to add solutions of the troublesome elements to

aliquots of the stable solution when needed for daily experiments.

Table 4.1 shows the concentrations of fission product elements in the HLLW, and the starting compounds and methods of dissolution used to prepare the synthetic waste solution.

Table 4.1. Preparation of synthetic high-level waste solution

Element	Quantity (g/liter)	Chemical compound	Remarks
Sr	0.163	$Sr(NO_3)_2$	Dissolved in water
In	2.47×10^{-3}	In_2O_3	Dissolved in 2.9 M HNO_3
Cd	0.017	$Cd(NO_3)_2$	Dissolved in water
Cs	0.482	$CsNO_3$	Dissolved in 2.9 M HNO_3
Se	9.89×10^{-3}	Metal	Dissolved in 9.75 M HNO_3
Ba	0.332	$Ba(NO_3)_2$	Dissolved in water
Te	0.112	Metal	Dissolved in 9.75 M HNO_3
Mo	0.680	$(NH_4)_6Mo_1O_{24}\cdot 4H_2O$	Dissolved in 2.9 M HNO_3
Sn	9.89×10^{-3}	Metal (20 mesh)	Dissolved in 2.9 M HNO_3
Ag	0.012	$AgNO_3$	Dissolved in water
Zr	0.724	$ZrO(NH_3)_2\cdot 2H_2O$	Dissolved in 2.9 M HNO_3
Br	0.003	$NaBrO_3$	Dissolved in water
I	0.053	HIO_3	Dissolved in water
As	1.855×10^{-5}	As_2O_3	Dissolved in water
Sb	2.47×10^{-3}	Metal	Dissolved in 9.75 M HNO_3
Pd	0.282	Sponge	Dissolved in conc. HNO_3
Rh	0.077	$Rh(NO_3)_3$	Dissolved in 2.9 M HNO_3
Rb	0.066	$Rb(NO_3)_3$	Dissolved in 2.9 M HNO_3
Ru	0.426	$RuNO(NO_3)_3$	Dissolved in 2.9 M HNO_3
La	0.254	$La(NO_3)_3\cdot 6H_2O$	Dissolved in water
Y	0.093	$Y(NO_3)_3\cdot 6H_2O$	Dissolved in 2.9 M HNO_3
Nd	0.816	$Nd(NO_3)_3\cdot 6H_2O$	Dissolved in water
Pr	0.239	$Pr(NO_3)_3\cdot 5H_2O$	Dissolved in 2.9 M HNO_3
Ce	0.492	$Ce(NO_3)_3\cdot 6H_2O$	Dissolved in 2.9 M HNO_3
Sm	0.177	$Sm(NO_3)_3\cdot 6H_2O$	Dissolved in 2.9 M HNO_3
Gd	0.024	$Gd(NO_3)_3\cdot 6H_2O$	Dissolved in 2.9 M HNO_3
Eu	0.034	Eu_2O_3	Dissolved in 2.9 M HNO_3
Fe	0.140	$Fe(NO_3)_3\cdot 9H_2O$	Dissolved in 2.9 M HNO_3
Cr	0.024	$Cr(NO_3)_3\cdot 9H_2O$	Dissolved in 2.9 M HNO_3
Ni	9.28×10^{-3}	$Ni(NO_3)_2\cdot 6H_2O$	Dissolved in 2.9 M HNO_3

5. AMERICIUM-CURIUM RECOVERY USING INORGANIC ION EXCHANGE MEDIA

D. R. Tallant (Sandia Laboratories)

The objective of this study is to determine the usefulness of certain inorganic ion exchange media for separating the trivalent actinides and lanthanides. During the first year, feasibility will be determined. If successful, flowsheets will be developed during the second year.

During the first quarter of FY 1977, the research plan was developed, quantities of candidate ion exchange materials were prepared, capital equipment was requisitioned, and preliminary studies of ion exchange material properties were carried out.

As now envisioned, the project will proceed in three phases. The initial phase will involve batch equilibration studies on titanate, niobate, and zirconate ion exchange materials. The goal is to survey a wide range of possible ion exchange materials (titanates, niobates, and zirconates with different barrier ions) for differences in affinities for actinide and lanthanide ions, and for stability in feed solutions of high nitric acid content. The batch equilibration approach allows a maximum number of studies to be carried out under closely controlled conditions without complications from column flow and kinetic effects. Solutions containing stable lanthanide nuclides will be contacted with an ion exchange material. Lanthanide ions remaining in solution will be analyzed by optical emission spectroscopy using an inductively coupled plasma source, allowing distribution coefficients between the ion exchanger and the solution to be calculated. Analogous studies using americium and curium, which may be analyzed by radioactive measurements, will yield distribution coefficients for these ions.

The most promising ion exchange materials determined by the equilibration studies will be utilized in the second phase of this program. Phase two will involve ion exchange column loading and elution of waste simulant solutions. The goal is to perform actual separations of lanthanide and actinide ions while determining the effects of column flow rates, eluents, and fission products in the feed solution on the degree of separation achieved. Pretreatment of the feed solution with inorganic ion exchangers (e.g., to remove fission products and the bulk of the lanthanides) will be considered during this phase.

Assuming that the first two phases of the project yield an ion exchange material suitable for lanthanide-actinide partitioning, the third phase will test the materials and procedures developed on partitioning from actual high-level waste. Time constraints may limit these studies in FY 1977, in which case flowsheets will be provided based on simulant studies. Preliminary studies have shown that the sodium forms of titanate, niobate, and zirconate materials exchange quantitatively with hydrogen ions even in moderately concentrated nitric acid. Therefore, H^+ is also being considered as a barrier ion.

During the second quarter of FY 1977, equilibration studies were carried out on titanate, niobate, and zirconate ion exchange materials to determine their stability in acid media and their affinities for candidate barrier ions and selected rare earth ions.

The acid stabilities (Table 5.1) were determined by equilibrating weighed portions of inorganic ion exchange materials with solutions of varying nitric acid concentration. The amount of titanium, niobium, or zirconium found in solution after equilibration indicates the extent of

dissolution of the ion exchange material. Vacuum-dried (V) titanates and zirconates show considerable dissolution at higher acid concentrations, but the fired (F) forms resist dissolution even when in prolonged contact with 0.5 M HNO_3. Fired titanates and zirconates retain 60% and 80%, respectively, of their unfired ion exchange capacities. Dissolution of both fired and vacuum-dried niobates is negligible over the pH range for which data are presented. The vacuum-dried niobate form is preferred since firing destroys most of its ion exchange capacity.

Table 5.1. Stability of inorganic ion exchangers

Exchanger	Percent dissolution of central ion			
	pH 7[a] or greater	0.02 M HNO_3[b]	0.1 M HNO_3[b]	0.5 M HNO_3
Sodium titanate:				
(F)[c]	—	—	—	0.55
(V)[d]	<0.007	<0.007	7.5	32
Sodium niobate:				
(F)	—	—	—	<0.002
(V)	<<1	<<1	<<1	0.001
Sodium zirconate:				
(F)	—	—	—	0.9
(V)	<0.02	<0.02	0.05	3.7

[a]24-hr equilibration.

[b]48-hr equilibration.

[c](F) - fired at 700°C.

[d](V) - vacuum-dried only.

Sodium titanate was converted to barrier ion form by equilibration with candidate barrier ions (Ba^{2+}, Cu^{2+}, Pb^{2+}, Zn^{2+}, Cr^{3+}, Fe^{3+}) at neutral pH. In 0.5 M HNO_3, none of these ions was retained by the titanate ion exchange material. Only the chromic and ferric titanates

remained in barrier ion form in 0.05 M HNO_3. These results indicate that barrier ion forms of the titanates can be effectively used only in neutral or dilute acid solutions.

The affinities of titanate, niobate, and zirconate ion exchange materials for rare earth (R.E.) ions in moderate nitric acid concentrations were investigated by further equilibration studies (Table 5.2).

Table 5.2. Results obtained in rare-earth equilibration studies[a]

Form of ion exchanger	Acid medium	Fraction of R.E.$^{3+}$ retained on ion exchanger			
		La^{3+}	Nd^{3+}	Pr^{3+}	Y^{3+}
Titanates:					
Na[b]	0.5 M HNO_3	0.07	<0.01	<0.04	0.10
Cr	0.05 M HNO_3	0.07	<0.04	<0.04	0.19
Fe	0.05 M HNO_3	0.10	<0.04	<0.04	0.20
Niobate:					
Na[b]	0.05 M HNO_3	0.10	<0.01	<0.04	<0.03
Zirconate:					
Na[b]	0.05 M HNO_3	0.05	<0.01	<0.04	<0.03

[a]Experiments consisted of 5 meq of ion exchanger, 1 meq of total R.E.$^{3+}$, and 100 ml of solution.

[b]Fired at 700°C.

Results obtained during work on the Sandia Solidification Process indicate that titanate, niobate, and zirconate ion exchange materials have high affinitives for R.E. ions at approximately neutral pH. The small take-up of these ions by titanates, niobates, and zirconates in moderate acid (Table 5.2) implies that R.E. ion exchanger affinities have a strong pH dependence.

Investigations into the relative affinities of americium, curium, and rare-earth ions for titanate, niobate, and zirconate materials as a function of pH are now being planned or are in progress. Differences in these affinities may allow selective elution of the components of Purex waste by pH adjustment.

6. RECOVERY ALTERNATIVES APPLICABLE TO WASTE STREAMS

E. P Horwitz, W. H. Delphin, G. W. Mason, C. A. A. Bloomquist, H. Griffin, S. Lewey, and M. Steindler (Argonne National Laboratory)

This task focuses on processing alternatives for recovering actinides and technetium from high-level liquid waste. Additional work will examine alternatives for separating the lanthanides from the trivalent actinides and for recovering actinides from salt wastes.

6.1 Summary

A tentative conceptual process sequence for the removal of Np, Pu, Am, Cm, and Tc from high-level liquid waste (HLLW) is presented. The process involves four basic steps: (1) removal of Np, Pu, and Tc using tricaprylmethylammonium nitrate ($TCMA \cdot NO_3$) in a liquid-liquid chromatography (LLC) mode; (2) extraction of interfering elements such as Zr, Mo, Gd, Y, and U using di(2-ethylhexyl) phosphoric acid (HDEHP); (3) extraction of Am, Cm, and rare earths with di(hexoxyethyl) phosphoric acid (HDHoEP); and (4) separation of Am and Cm from the rare earths. The Zr, Mo, Gd, Y, and U, together with the rare earths separated from Am and Cm, are returned to the HLLW raffinate from step 3.

A flowsheet for the removal of Np, Pu, and Tc from the HLLW is presented. The process is based on the high extractabilities of Np(IV), Pu(IV), and Tc(VII) using $TCMA \cdot NO_3$. All fission products and corrosion products are poorly extracted. The Tc(VII) is separated from Np and Pu using 6 M HNO_3, and the Np and Pu are stripped using 1 M formic acid--0.1 M HNO_3.

Flowsheets are shown for the extraction of certain fission products, namely, Zr, Mo, Y, and U, from HLLW by HDEHP and for the subsequent extraction of Am and Cm from the resultant raffinate by HDHoEP. The latter process is based on the high extractabilities of Am and Cm by HDHoEP from nitric acid solutions up to 2 M in concentration.

6.2 Introduction

The treatment of high-level waste to remove long-lived nuclides has been proposed as a method for simplifying waste management procedures. This partitioning is usually aimed at treatment of the liquid waste from the first-cycle processing of spent fuel by solvent extraction. A program has been initiated by ERDA and managed by ORNL to demonstrate partitioning as a feasible technology option in the management of nuclear waste.

The present program is directed toward an examination of the feasibility of recovering macro amounts of long-lived actinides, Np, Pu, Am, and Cm, and fission product Tc from commercial high-level waste (HLLW), using various quaternary ammonium nitrates and dialkylphosphoric acid extractants. The process is divided into two distinct parts. The first part involves the extraction of Np, Pu, and Tc from synthetic HLLW solution using a trialkylmethylammonium nitrate salt in diethylbenzene. This separation will be tested in high-speed liquid-liquid extraction (LLE) and high-speed (LLC) modes. Emphasis will be placed on decontamination of these nuclides from unwanted fission products and corrosion products and on efficient and rapid stripping of Np, Pu, and Tc from the extractant. The second part involves the extraction of Am and Cm from the raffinate of the first part, using a dialkyl phosphoric acid extractant.

Investigations will concentrate on efforts to lower the distribution coefficients of Zr, Mo, and U using complexing agents such as oxalate and fluoride ions in order to improve extractant selectivity for Am and Cm. An alternative approach that has been included in preliminary flowsheets will use an intermediate extraction of Zr, Mo, and U in order to eliminate their interference with the Am and Cm extraction in the second part. Emphasis is placed on achieving a high recovery of the desired nuclides with a minimum transfer of unwanted fission products and corrosion products (e.g., Cr, Mo, Fe). A final separation of Am and Cm from coextracted rare earths is planned.

The chemical information developed in the experimental program will be supplemented by several types of on-going reviews aimed at evaluation of the feasibility of these methods. Initial efforts will collect existing process-related information on systems likely to be studied (e.g., radiation stabilities and the properties of degradation products, solubilities in various solvents, corrosion of and compatibility with materials of construction, commercial availability or estimated costs to produce reagents, safety-related properties, etc.). Preliminary conceptual flowsheet designs will be drawn as soon as sufficient extraction equilibria data are available. These flowsheets will serve to focus on specific areas where additional data are needed.

6.3 Experimental

6.3.1 Extractants

The quaternary amine employed in this study was TCMA·NO_3. A technical grade of this amine (called Aliquat-336 chloride) was obtained from General

Mills, Inc. This amine was either used as received (usually for LLC studies) or purified by LLE using a cyclohexane--50:50 water:acetonitrile system. The quaternary amine remains in the acetonitrile phase, whereas the tertiary and lower amines concentrate in the cyclohexane phase. Two batch extractions (org.:aq. = 1) of the acetonitrile-water phase with cyclohexane are normally employed. After the extraction, the acetonitrile-H_2O is removed from the quaternary amine by means of a commercial rotary evaporator.

The HDEHP was obtained from Union Carbide, Inc., and purified using the method suggested by Peppard.[1] The HDHoEP was synthesized and purified following the procedure of Peppard.[2]

6.3.2 Preparation of bed material and column packing

Porasil®* was used as the inert support for preparing the LLC columns. Porasil consists of spherical, porous silica beads 37 to 75 μm in diameter. The material was hydraulically graded[3] into two particle size fractions: 37 to 60 μm and >60 μm. The 37- to 60-μ-diam fraction was used to prepare the LLC columns. Porasil is available in four pore size ranges from <100 to <1500 Å in diameter. Porasil C, which has a pore diameter range of 200 to 400 Å (Hg intrusion) and a surface area of 50 to 100 m^2/g (BET), was used in this study. The chromatographic properties of other Porasils are being investigated.

The Porasil support was made hydrophobic by refluxing 24 hr in hexamethyldisilazane. Organic extractant, 30 vol % TCMA·Cl in diethylbenzene (DEB), was applied to the Porasil using the conventional solvent

---

*Product of Waters Associates, Milford, Mass.

evaporation technique.[4] Optimum loading of the support (50 wt %) was ascertained experimentally by successful approximations. The overloaded support is wet, whereas the optimum or underloaded support is dry. The resultant dry column material was easily wetted for slurry packing of the column by vortexing with 0.1 M HCl. Columns were prepared by slurry packing under pressure.[4] Column bed density (i.e., the number of grams of column material per milliliter was measured by extruding, drying, and weighing the contents of a column of known volume.

6.3.3 Measurements of K_d, and column run procedure

Distribution ratio measurements were performed in the conventional manner using standard radiometric assay and counting techniques. The K_d measurements made at 50°C were carried out by intermittent thermostating and vortexing small culture tubes containing the two phases.

The equipment utilized in the chromatographic experiments and the general column run procedure are described in a previous paper.[5] Although a medium-pressure (500 psi, 3.45×10^6 Pa) LC pump, valves, and tubing were employed, the pressure drop across the column during high-speed column runs did not exceed 175 psi (1.21×10^6 Pa).

6.4 Results and Discussion

6.4.1 Process sequence

A tentative conceptual process sequence for the removal of Np, Pu, Am, Cm, and Tc from high-level liquid waste is shown in Fig. 6.1. The process involves four basic steps. First, Np(IV), Pu(IV), and Tc(VII) are selectively removed from the HLLW using the quaternary amine TCMA·NO_3

ORNL DWG. 77-9185

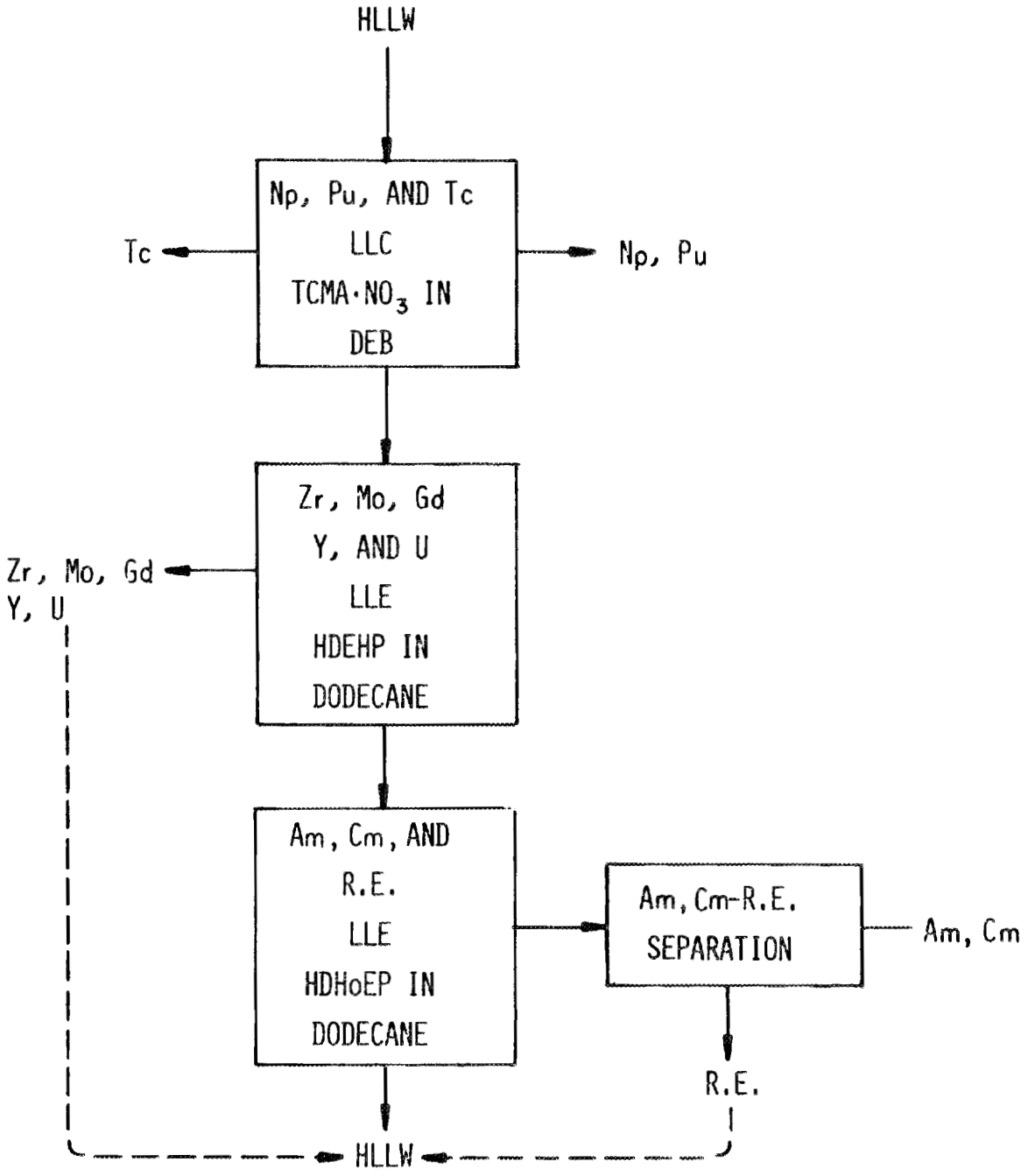

Fig. 6.1. Conceptual flowsheet illustrating processing sequence to partition the actinides and lanthanides from HLLW.

in diethylbenzene (DEB). The second step involves LLE of the HLLW using HDEHP in dodecane. This extractant removes Zr(IV), Mo(VI), Gd(III), Y(III), and U(VI), which interfere (to a greater or lesser extent) with the subsequent extraction of Am and Cm. In the third step, the Am(III) and Cm(III), together with the remaining rare earths (which are primarily La and Eu), are extracted with HDHoEP in dodecane. The LLE in step 3 requires a prior evaporation or dilution of the HLLW in order to lower the H^+ concentration to $\sim$1 M. After removal of the Am and Cm from HLLW, the Zr, Mo, Gd, Y, and U that were extracted in step 2 are combined with the raffinate from step 3. The final phase of the process involves the separation of Am and Cm from rare earths; however, the details of this step have not yet been developed.

The processing sequence shown in Fig. 6.1 is based on very preliminary laboratory investigations. Some of the steps in the process have not been experimentally verified, although every step appears feasible based on past experience. Experimental work, particularly with gross concentrations of certain fission products and with synthetic waste solutions, remains to be done. The radiation stability and subsequent cleanup of the extractants, as well as the stability of the LLC columns, remain to be studied, even though some preliminary information concerning these parameters is available

6.4.2 Removal of Np, Pu, and Tc with TCMA·NO_3 in DEB

A flowsheet for the removal of Np, Pu, and Tc from HLLW using an LLC column containing 30 vol % TCMA·NO_3 in DEB as the stationary phase is shown in Fig. 6.2. The feed solution for this process is the HAW fraction from the Purex process flowsheet described in ref. 6. This

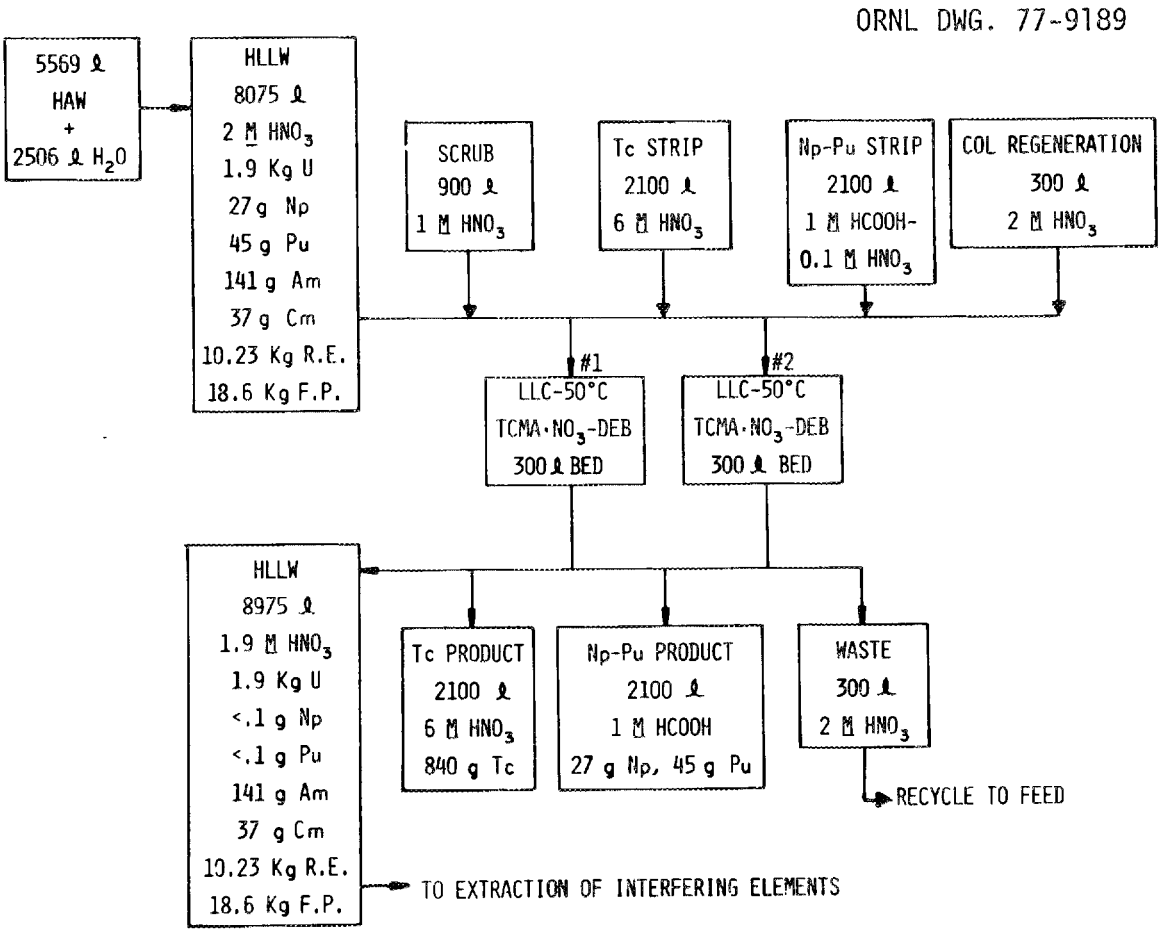

Fig. 6.2. Conceptual flowsheet for Np, Pu, and Tc removal from HLLW using TCMA·NO_3-DEB columns. Basis, 1 tonne of heavy metal.

waste stream (i.e., the HAW) has a volume of 5569 liters per tonne of heavy metal (i.e., U + Pu) and is 2.9 M in HNO_3. The quantities of fission products and actinide elements were for a typical LWR fuel irradiation to 33,000 MWd/tonne based on 0.5% loss of plutonium to the HAW.[6]

The flowsheet in Fig. 6.2 is based on the high extractability of Np(IV), Pu(IV), and Tc(VII) by TCMA·NO_3. Figure 6.3 shows some distribution ratios* determined in this program for tetravalent and hexavalent actinides and Tc(VII), together with selected fission products, using 30 vol % TCMA·NO_3 in DEB. The fission product data were obtained from Koch et al.,[7] who used Solvesso®** as a diluent. Koch also published actinide data similar to those determined in this work by using TCMA·NO_3 in Solvesso. The tetravalent actinides and Tc(VII) are present in the TCMA·NO_3 phase as $(R_4N)_2Pu(NO_3)_6$ and R_4NTcO_4; uranium occurs as $R_4NUO_2(NO_3)_3$. These stoichiometries were determined in this work by means of loading experiments and extractant dependencies.

In the first step of the flowsheet shown in Fig. 6.2, the feed solution is diluted with H_2O to decrease the acidity to 2 M HNO_3 in order to increase the K_d of Tc. No valence adjustment for Np and Pu is shown, although such an adjustment might be necessary and would probably be done with N_2O_4. However, the observed K_d's of Pu and Np from 2 M HNO_3 using 30 vol % TCMA·NO_3 in DEB are $>10^2$ without any valence adjustment. One reason for the high K_d's from HNO_3 without a separate valence adjustment

---

*$K_d = \frac{\text{concentration of nuclide in organic phase}}{\text{concentration of nuclide in aqueous phase}}$,

**Product of Exxon Chemical Co., Houston, Texas.

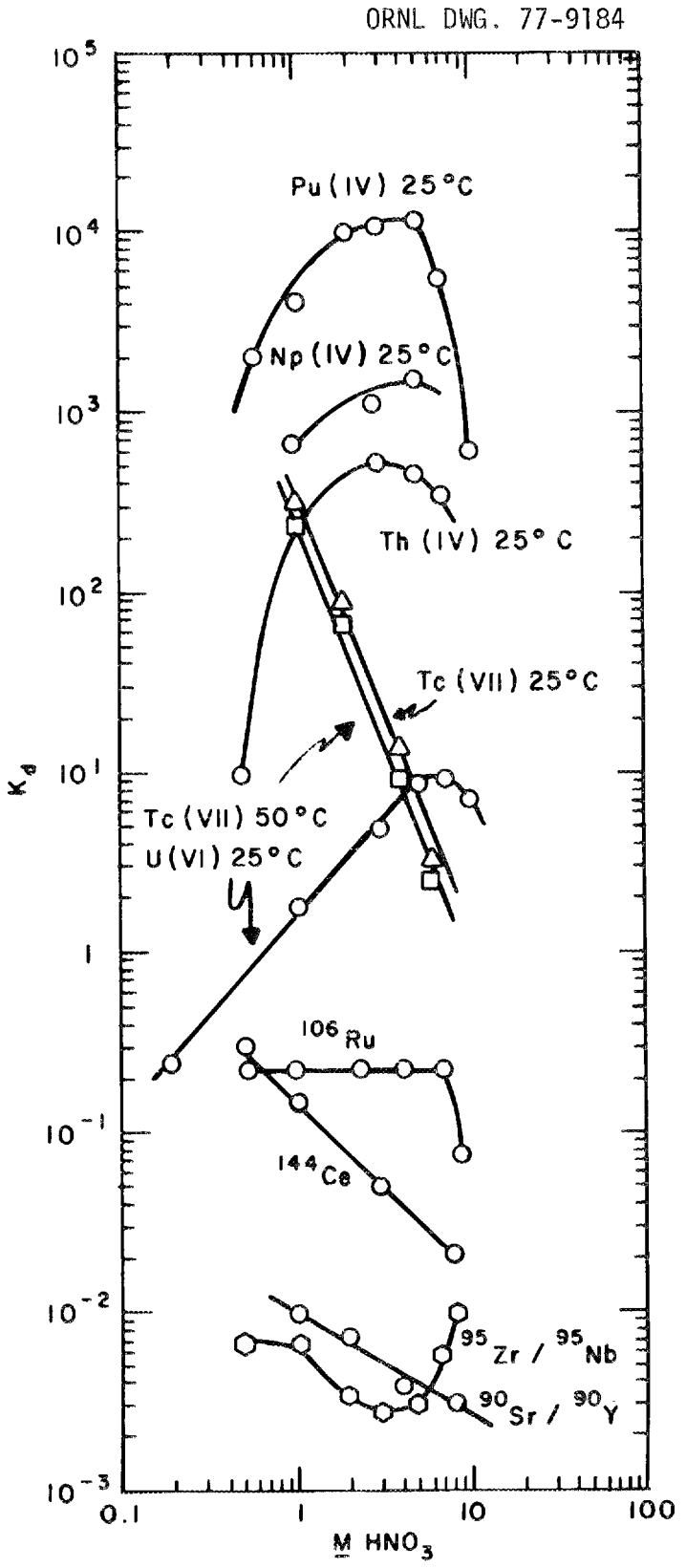

Fig. 6.3. Nitric acid concentration vs distribution ratios for selected actinides and fission products between 30 vol % TCMA·NO_3 in DEB and HNO_3.

step* is that Pu(VI) and Np(VI), and possibly Np(V), are reduced to the tetravalent state by the amine extractant unless a strong holding oxidant is present.

The LLC columns shown in Fig. 6.2 consist of a stationary phase of 30 vol % (0.5 M) TCMA·NO_3 in DEB absorbed on totally porous spherical silica particles 35 to 60 μm in diameter. The optimum pore size of the silica particles has not been determined. The maximum liquid loading of stationary phase on the particles is a function of the pore size but will probably be in the range of 45 to 50 wt %.

Full-scale process columns would have 300-liter bed volumes (2234 cm^2 x 134 cm), or dimensions of 21 in. ID x 52.8 in. long, and would be operated at 50°C. Table 6.1 gives the column dimensions, capacity (50 wt % extractant on support), and quantities of Np, Pu, and Tc extracted. It is interesting to note that Tc is the major molar constituent and that ∿94% of the TCMA·NO_3 complexed is used to extract TcO_4^-. Liquid loading experiments carried out in the LLE mode with 30 vol % TCMA·NO_3 in DEB indicated no solubility or phase separation problems on extracting macro concentrations of TcO_4^-, even when the organic phase was saturated (i.e., 50 g of Tc per liter).

The flowsheet in Fig. 6.2 shows two LLC columns. The reason for using a two-column system is that continuous process operation can be obtained by alternating the loading and eluting cycles between two columns. Table 6.2 shows estimates of loading and eluting cycle times for a

---

*The oxidation of Pu(III) by HNO_3 is assumed. A detailed description of the treatment of high-level waste solutions as observed under process conditions (e.g., presence of insoluble materials, mutiple-valence state of important elements, etc.,) will be presented in subsequent reports.

Table 6.1. Column dimensions and capacity consumption

Column bed density	0.754 kg per liter of bed volume
Volume of stationary phase	0.435 liter per liter of bed volume
$TCMA \cdot NO_3$ in DEB	30 vol % (0.5 M)
Moles of $TCMA \cdot NO_3$	0.217 per liter of bed volume
Column size	2234 cm^2 x 134 cm (21.0 in. ID x 52.8 in. long)
Bed volume	300 liters
Total capacity	65.10 moles of $TCMA \cdot NO_3$ per column

Quantities of Tc, Np, Pu to be extracted from HLLW/MTHM

Element	Weight (g)	Moles	Moles of $TCMA \cdot NO_3$ consumed
Tc	840	8.49	8.49
Np	27	0.114	0.228
Pu	45	0.188	0.376

Total capacity consumed = 6.98%

Table 6.2. Loading and elution cycles (4 hr/cycle) for TCMA·NO_3-DEB columns (Basis: 1 tonne of heavy metal)

Column 1				Column 2			
Time (min)	Solution	Volume (liters)	Flow rate (liters/min)	Time (min)	Solution	Volume (liters)	Flow rate (liters/min)
120	HLLW	4038	33.7	15	1 M HNO_3	450	30
				50	6 M HNO_3	1050	21
				50	1 M HCOOH	1050	21
				5	2 M HNO_3	50	30
15	1 M HNO_3	450	30	120	HLLW	4038	33.7
50	6 M HNO_3	1050	21				
50	1 M HCOOH	1050	21				
5	2 M HNO_3	150	30				

two-column system. The pressure drop at the maximum linear flow velocity (30 cm/min) was measured at 2.3×10^6 Pa (334 lb/in.^{2}).

The decontamination of the HLLW from Np, Pu, and Tc can only be estimated based on simple laboratory experiments. The decontamination factor (DF) for Pu is influenced by the amount of "nonextractable" plutonium present in the waste solution. If nonextractable plutonium is not considered, the DF should be $\sim 10^3$ for Pu and approximately the same for Np and for Tc. Experimental column runs have indicated no major problem in stripping Tc and Np-Pu from the TCMA·NO_3 in DEB columns. The flow direction of the stripping operation would be the opposite of the loading operation in order to improve column cleanup.

The process shown in Fig. 6.2 can also be carried out entirely by conventional LLE with some modification. Insufficient data exist at this time to decide which technique would give the best results for the least cost.

6.4.3 Extraction of interfering fission products using HDEHP

A flowsheet for the removal of Zr, Mo, Y, and U, and possibly Sb, Sn, and Fe (from corrosion from HLLW), by LLE using HDEHP in dodecane is shown in Fig. 6.4. The feed solution for this step is the column eluate (or raffinate if LLE is used) from the loading and acid scrub cycles of the Np, Pu, and Tc extraction step. This flowsheet is based on the high extractabilities of tetravalent and hexavalent metal ions, Y, and heavy rare earths by HDEHP.[8] No valence adjustment or acidity change is required for the extraction, using 0.5 M HDEHP in dodecane. Most published K_d values using HDEHP were determined at room temperature. Since ambient temperature during the LLE steps would probably lie in the 40 to 50°C range,

ORNL DWG. 77-9191

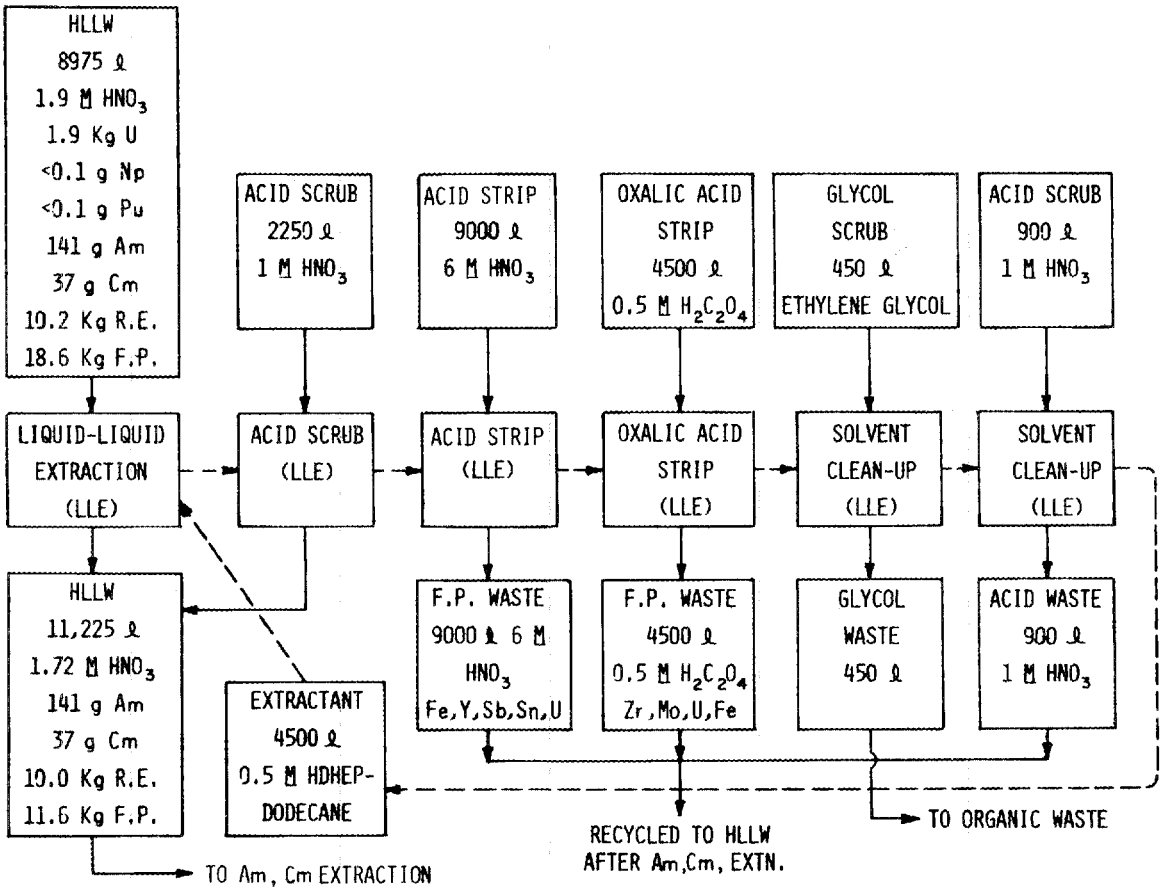

Fig. 6.4. Conceptual flowsheet for the extraction of interfering fission products from HLLW using HDEHP-dodecane. Basis: 1 tonne of heavy metal.

additional K_d's for Zr, Mo, U, and Y will be required at 50°C. However, the K_d's for these elements from 2 M HNO_3 at 25°C are so high (except for Y) that the influence of temperature will not alter the overall flowsheet significantly. More important is the existence of the polynuclear compounds fo Zr and their influence in the chemical behavior of this element during LLE. Simulation of HLLW by dissolution of small samples of irradiated fuel, followed by one cycle of Purex extraction, is planned to elucidate the behavior of both zirconium and ruthenium.

As shown in Fig. 6.4, the fission products extracted by HDEHP are stripped successively with 6 M HNO_3 and 0.5 M $H_2C_2O_4$ and recycled to the HLLW stream after the Am and Cm extraction process. The uranium present in the oxalate strip* could be separated from the Zr and Mo by dissolving in 8 M HNO_3 and extracting with 30 vol % TCMA·NO_3 in DEB.

6.4.4 Extraction of Am, Cm, and rare earths using HDHoEP

A flowsheet for the removal of Am, Cm, and rare earths from HLLW waste by LLE using HDHoEP in DEB or diisopropylbenzene (DIP) is shown in Figs. 6.5 and 6.6. These flowsheet are based on the high distribution ratios obtainable from nitric acid solutions, even up to 2 M, using HDHoEP. Figure 6.7 shows extractant dependencies in heptane (dodecane diluent gives the same value) for Am and Eu from 1 M as well as from 4 M HNO_3. Figure 6.8 shows the extractant dependency of Cm and Pm from 4 M HNO_3.

Slopes of the K_d curves decrease with increasing concentration, from ∿1 to 1.5 at low extractant concentrations to <1 at high extractant concentrations. These data clearly indicate an increase in association

---

*Very little uranium would be present in the 6 M HNO_3 strip.

ORNL DWG. 77-9190

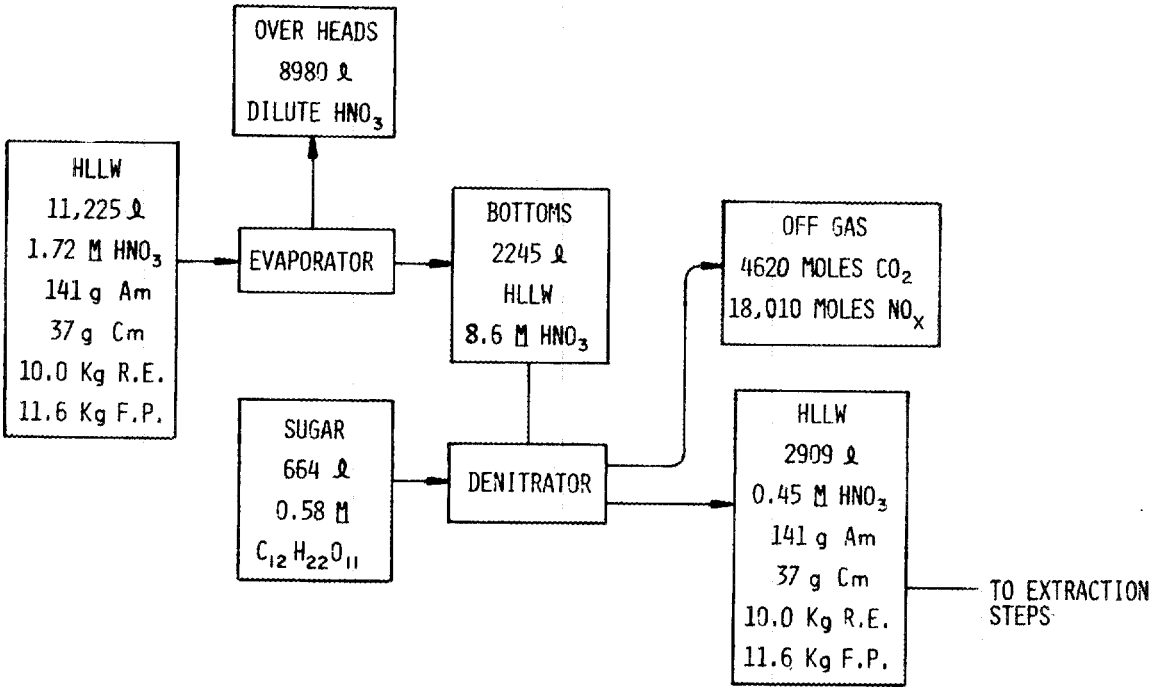

Fig. 6.5. Conceptual flowsheet for Am, Cm, and rare-earth removal from HLLW using HDHoEP in DEB (Part 1). Basis: 1 tonne of heavy metal.

ORNL DWG. 77-9188

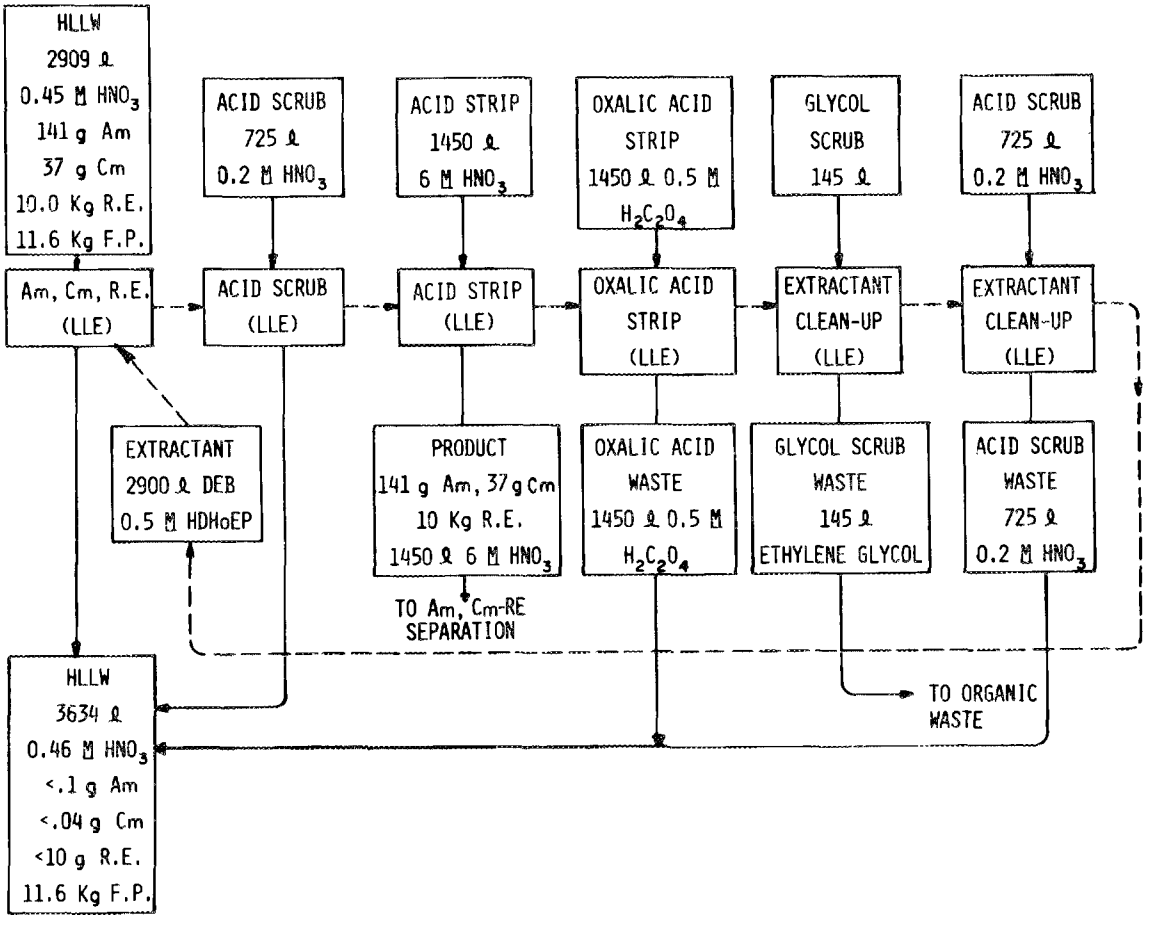

Fig. 6.6. Conceptual flowsheet for Am, Cm, and rare-earth removal from HLLW using HDHoEP in DEB (Part II). Basis, 1 tonne of heavy metal.

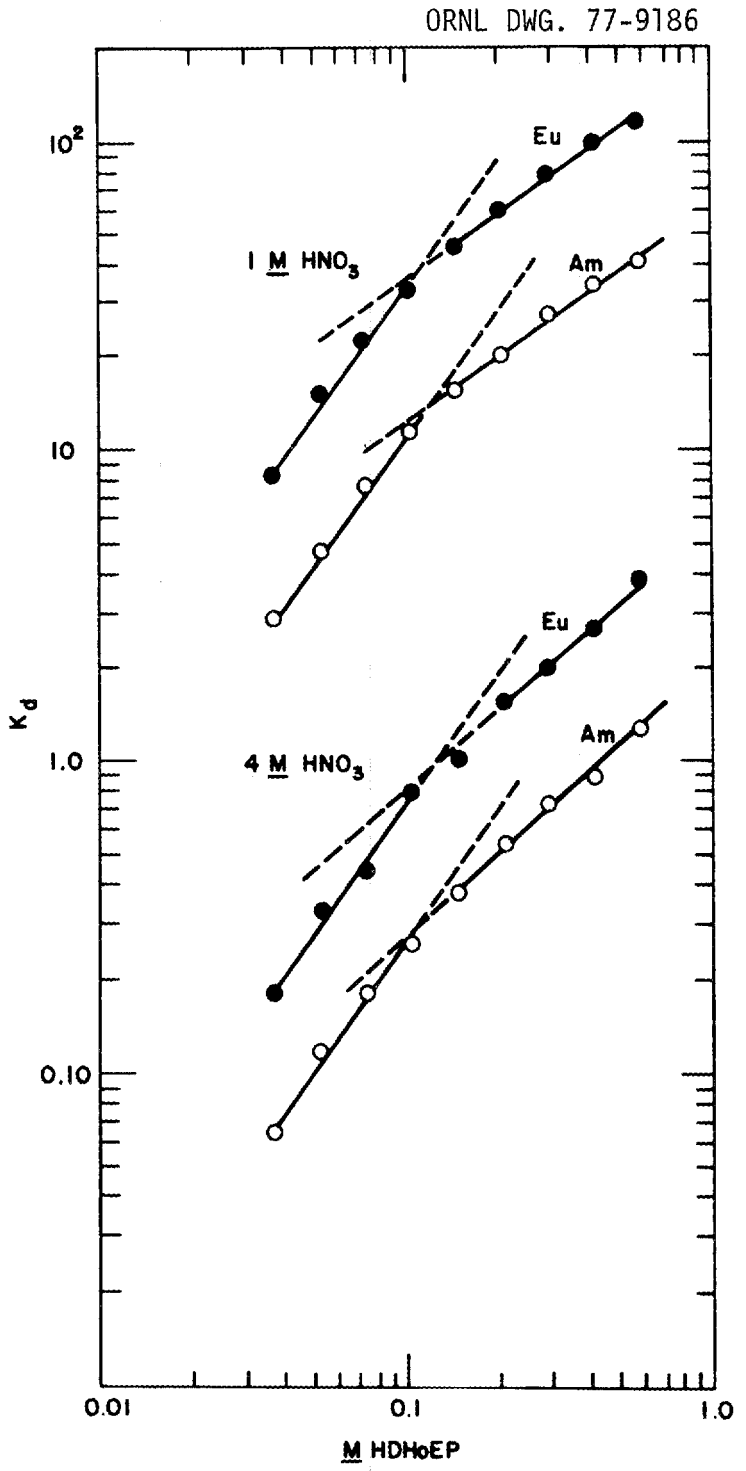

Fig. 6.7. Distribution coefficients of Eu(III) and Am(III) for various concentrations of HDHoEP in heptane and 1 M or 4 M HNO_3.

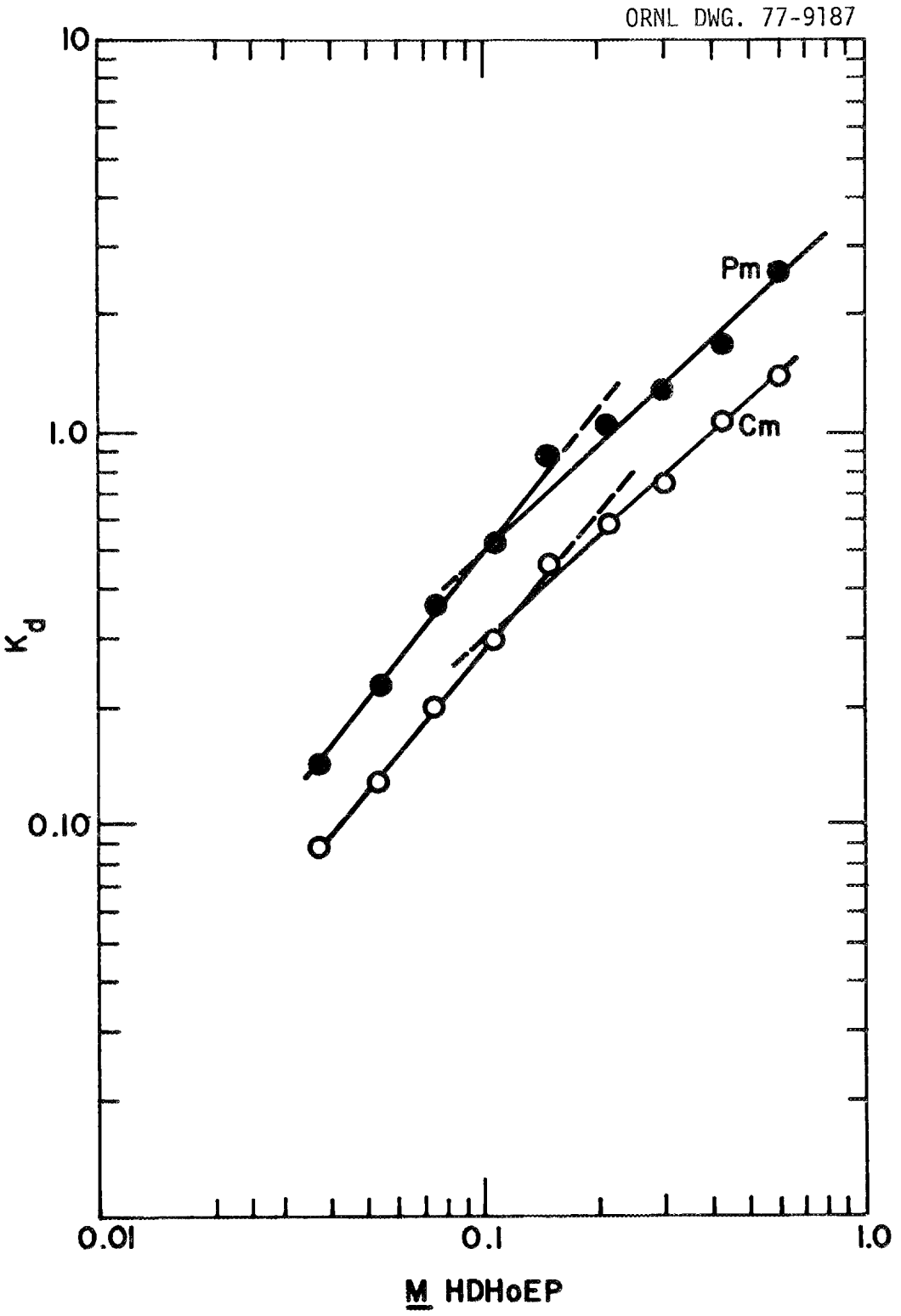

Fig. 6.8. Distribution coefficents for Pm(III) and Cm(III) between 4 M HNO_3 and various concentrations of HDHoEP in heptane.

of the HDHoEP with concentration, which is not surprising when compared with the behavior of other alkyl phosphoric acids. The presence of the ether linkage in the HDHoEP is, in all probability, responsible for the increase in association as compared with concentrated HDEHP-dodecane solutions. Acid dependencies show the expected slope of -3.5 (when ionic strength is not held constant) at low acidity. However, in the vicinity of 1.5 M HNO_3 the slope begins to decrease and reaches -2 at 4 M HNO_3. These results indicate that a $MNO_3{}^{2+}$ ion may be extracted by HDHoEP. Extraction of NO_3^- by HDEHP at high nitrate concentrations is well known. The following equilibria describe the extractions:

$$M^{3+} + n(HY)_m \rightleftarrows MH_{nm-}Y_{nm_3} + 3H^+$$

$$MNO_3{}^{2+} + n(HY)_m \rightleftarrows MNO_3H_{nm-2}Y_{nm} + 2H^+,$$

where HY is the acid HDHoEP, Y is the anion $DHoEP^-$, and m is the degree of association of the extractant.

In order to obtain process-related data, the extraction of Am^{3+} by HDHoEP in dodecane was studied, using a two-level, three-factorial design. The three independent variables and their levels were acidity (0.525 and 2.13 M HNO_3), extractant concentration (0.5 and 1.0 M), and temperature (25 and 50°C). A prediction model equation for the variation of the K_d as a function of acidity, extractant concentration, and temperature was dervied from the results of the factorial experiments. The equation is as follows:

$$\log K_d = 1.59 - 0.942X_1 + 0.103X_2 - 7.4 \times 10^{-3}X_3 + 0.0304X_1X_2 - 0.0237X_1X_3 + 0.0074X_2X_3,$$

where

$$X_1 = \frac{\log[H+] - 0.024}{0.304},$$

$$X_2 = \frac{\log[Ex] + 0.150}{0.150},$$

$$X_3 = \frac{[1/T^{o}K] - 3.23 \times 10^{-3}}{-1.3 \times 10^{-4}}.$$

Distribution ratios (K_d) of Am(III) range from 5.8 in 2.13 M HNO_3 to 300 in 0.525 M HNO_3, using 1 M HDHoEP at 50°C. These K_d's are very high, which is favorable for the extraction of Am and Cm from HLLW; however, stripping these ions from the organic phase is difficult. Decreasing the extractant concentration to the 0.2 to 0.4 M range alleviates the back-extraction problem to some degree. However, a better solution may lie in taking advantage of the diluent effect shown with dialkyl phosphoric acid extractants.[9] Preliminary measurements of Am and Eu distribution ratios using HDHoEP in DIB have shown decreases in K_d by a factor of 8 to 0.2 M HDHoEP. However, the K_d's of Am and Eu using 1 M HDHoEP in DIB were comparable to those obtained in the dodecane diluent. Therefore, there appears to be a larger extractant dependency in the aromatic diluent.

The flowsheet in Fig. 6.6 is based on the extraction of Am and Cm from 0.45 M HNO_3 using 0.5 M HDHoEP in DEB. Prior evaporation and denitration (Fig. 6.5) are used to reduce the acidity of the HLLW.

Approximately 72 moles of Am, Cm, and rare earths (Ce-Eu) will be extracted by the HDHoEP. This extraction will require 432 moles of HDHoEP (extractant:M^{3+} ratio = 6). The flowsheet in Fig. 6.6 shows 1450 moles of HDHoEP before extraction, which will leave 1018 moles of HDHoEP after extraction. An extractant concentration of 0.35 M of uncomplexed HDHoEP in DEB after extraction should have a K_d from Am of ∿6.5,

thus ensuring a high decontamination of the HLLW using ten stages. These flowsheets are highly tentative, and other possibilities such as the direct extraction of Am and Cm from 1.72 M HNO_3 using HDHoEP in dodecane may be a better approach. These options will be examined more closely using synthetic HLLW waste.

6.5 Conclusions

A four-step preliminary flowsheet for the separation and isolation of Np, Pu, Am, Cm, and Tc from high-level waste has been developed on the basis of either known or reasonably probable distribution coefficients. The initial separation of Tc and a Np-Pu fraction from the HLLW has been tested on a laboratory scale and appears to be functional. The removal of interfering elements in the second step is designed on the basis of reported distribution data but has not been completely defined. Extraction of the Am-Cm fraction, accompanied by R.E. fission products, has been outlined, and the behavior of Am in HDHoEP-dodecane has been defined. Procedures for the extraction of Am-Cm appear to be available but are presently complicated by difficulties in stripping this fraction from the extractant. Additional work on this problem and the separation of Am-Cm from rare earths is in progress.

6.6 References for Section 6

1. D. F. Peppard, G. W. Mason, J. L. Maier, and W. J. Driscoll, "Fractional Extraction of the Lanthanides as Their Di-Alkyl Orthophosphates," J. Inorg. Nucl. Chem. 4, 334 (1957).

2. D. F. Peppard, G. W. Mason, and H. Griffin, J. Inorg. Nucl. Chem. 27, 1683 (1965).

3. E. P. Horwitz and C. A. A. Bloomquist, "High Speed Radiochemical Separations by Liquid-Liquid Chromatography Using a CSP Support: I: Performance of Quaternary Ammonium Chloride-3ipax System for the Elution of Cd(II) with HCl, "J. Chromatog. Sci. 12, 11 (1974).

4. E. P. Horwitz and C. A. A. Bloomquist, "The Preparation, Performance, and Factors Affecting Band Spreading of High Efficiency Extraction Chromatographic Columns for Actinide Separations," J. Inorg. Nucl. Chem. 34, 3851 (1972).

5. E. P. Horwitz, C. A. A. Bloomquist, and W. H. Delphin, "Radiochemical Separations by Liquid-Liquid Chromatography Using PSM Support," J. Chromatog. Sci. (in press) (1977).

6. W. D. Bond and R. E. Leuze, Feasibility Studies of the Partitioning of Commercial High Level Wastes Generated in Spent Nuclear Fuel Reprocessing: Annual Progress Report for FY-1974, ORNL-5012 (1975).

7. G. Koch, A. A. C. McKay, T. V. Healy, I. L. Jenkins, and A. Naylor (ed.), Solvent Extraction Chemistry of Metals, pp. 247-66, Chemical Rubber Co. Press, Cleveland, 1967.

8. G. Ghersini, pp. 68-133 in Extraction Chromatography, ed. by T. Braun and G. Ghersini, Elsevier, Amsterdam, 1975.

9. G. W. Mason, D. N. Metta, and D. F. Peppard, "The Extraction of Selected M(III) Metals by Bis 2-Ethylhexyl Phosphoric Acid in n-Heptane," J. Inorg. Nucl. Chem. 38, 2077 (1976).

7. ACTINIDE RECOVERY FROM COMBUSTIBLE WASTE

G. H. Thompson (Rockwell International, Rocky Flats Plant)

The objective of this task is to determine the recoverability of actinides from incinerator ashes. During the second year, the distribution of actinides through the preferred recovery system will be measured.

7.1 Summary

A preliminary literature survey has been completed, and a preliminary evaluation of common leaching and fusion methods shows that:

(1) Fusion with commonly used reagents dissolves >60% of the ash from the fluidized-bed incinerator process.

(2) Leaching with concentrated nitric acid dissolves 40 to 60% of the same ash.

Preparation of plutonium-contaminated ash is in progress. Leaching and fusion methods extant in the literature will be evaluated when this ash is available.

7.2 Introduction

The objective of this task is to evaluate methods for recovering actinides from incinerator ashes using current technology; that is, the scope of the work does not include development and testing of new methods. In addition, candidate processes should not preclude actinide recycle, cause high actinide losses to the off-gas, materially increase waste volumes, or have a deleterious effect on final waste forms being considered for long-term storage (concrete and glass). The ideal process

would involve leaching with nitric acid since this would permit immediate recycle to the modified Purex process envisioned for waste reprocessing. However, it is questionable whether nitric acid leaching can provide the desired level of actinide recovery, even if this chemical method is enhanced with physical methods such as ultransonic agitation. Therefore, it is probable that two processes will be required: a primary process to dissolve the actinides, and a secondary process to recover the actinides in a medium suitable for recycle. Because of this probability, no leaching or fusion methods have been excluded *a priori*. For example, although leaching or fusion with sulfate or sulfate-producing compounds is not desirable (sulfate is deleterious to glass), these methods are being investigated. If the amount of sulfate-containing waste is small compared with the overall amount to be fixed, such methods remain a viable option.

The ash to be leached is being produced by the fluidized-bed incineration (FBI) process. This process uses *in situ* neutralization of acid gases by the bed material (Na_2CO_3), catalytic afterburning, and gas filtration to produce a clean flue gas without aqueous scrubbing. A distinct advantage of this system is the lower operating temperature (500°C vs 800 to 1000°C for conventional incineration); this produces less refractory material.

The FBI process yields three types of ash products: ash from the fluidized bed (incinerator), recovered in the primary cyclone; ash from the catalytic afterburner which burns the flue gas, recovered in the secondary cyclone; and ash recovered from the porous stainless steel filters used to clean the gas stream prior to the HEPA filter system. These products are referred to as primary, secondary, and filter ash.

7.3 Experimental

7.3.1 Materials

The primary, secondary, and filter ash being used during this initial period is obtained from general trash burned in the pilot-scale FBI system. This ash contains no actinides or fission products; results of the analyses are shown in Table 7.1. All fusion and leaching agents are reagent-grade chemicals.

Table 7.1. Analyses (in wt %) of ash produced by burning general trash constituents

Ash	Element				Water-insoluble fraction
	Cl	C	Cr	Al	
Primary cyclone	4.2	18.2	0.42[a]	7.4	77.2
Secondary cyclone	5.7	1.6	3.50	14.3	88.7
Filter fines	6.7	12.7	2.78	18.3	94.3

[a]Presence of chromium in primary ash is not explained since no catalyst is used in the fluidized incinerator bed.

7.3.2 Procedure

All experiments were performed on ash which had been washed with distilled water to remove solubles and dried overnight at 110°C. For leaching experiments, 100 ml of leachant was added to 10 g of ash (liquid:solid ratio of 10:1). The mixture was refluxed for 2 hr; a total reflux condenser was used to prevent liquid loss. After cooling, the mixture was filtered or centrifuged and the residue washed with ∿500 ml of distilled water. The residue was dried overnight at 110°C, cooled in a desiccator, weighed, and the weight loss calculated.

Two leachants have been used. The first was concentrated HNO_3. The second was a mixture of concentrated sulfuric and nitric acids (95 and 5 vol % respectively). The latter is the acid composition used in the acid digestion process reported by Lerch and Cooley,[1] and additional HNO_3 was added at the rate of 5 ml of HNO_3 per half hour during the 2-hr leach (digestion) time.

For fusion experiments, 10 g of fusion agent was mixed with 1 g of ash (solid:ash ratio of 10:1). Fusion with basic materials were done in nickel crucibles, while fusions with acidic materials were done in quartz crucibles. The crucibles were placed in a muffle furnace and heated to $500^{o}C$ (heating rate, $\sim 2^{o}C/min$). The mass was heated at $500^{o}C$ for 1/2 hr. After the specified time the samples were removed, cooled in a desiccator, weighed, dissolved, washed, dried at $110^{o}C$, reweighed, and the percent weight loss calculated.

Ash samples were also fired to determine the weight loss attainable by this method. Weighed samples were fired in Alundum crucibles for 1 hr using a Meker burner. The crucibles were then placed in a desiccator to cool; after cooling, they were weighed, and the weight loss was calculated.

7.4 Results and Discussion

Results of the leaching, fusion, and firing experiments are shown in Table 7.2. The data are expressed as percent ash destroyed since this ash contains no radionuclides.

The concentrated nitric acid leach dissolved little of the ash. Although it is not possible to conclude at this time that nitric acid

Table 7.2. Ash destruction by leaching, fusion, and firing[a]

Method	Temperature (°C)	Time (hr)	Ash destroyed (wt %)		
			Primary	Secondary	Filter fines
15.7 M HNO_3 leach	Reflux	2	57	36	51
H_2SO_4-HNO_3 digestion (95% H_2SO_4)	Reflux	2	-39[b]	-30[b]	75
NaOH fusion	500	0.5	66	62	63
$KHSO_4$ fusion	500	0.5	65	66	65
$K_2S_2O_7$ fusion	500	0.5	69	75	69
Na_2O_2 fusion	500	0.5	80	75	70
Firing (Meker)	∿1250	2	37	44	18

[a]Ratio of leach to solid was 10; ratio of fusion agent to solid was also 10.

[b]Weight increased. Residue was difficult to wash and filter, and solidified into a glass-like mass upon drying.

leaching will not suffice (tests on contaminated ash are required), it appears that the desired recovery (≥99%) will not be achieved. The sulfuric-nitric acid digestion process reduced only the amount of filter fines residue. The residues from the primary and secondary ash actually increased in weight. However, this may be due to the difficulty experienced in washing and filtering (i.e., inadequate washing).

Fusion with NaOH, $KHSO_4$, $K_2S_2O_7$, and Na_2O_2 gave better results, destroying from 60 to 80% of the ash. The time and temperature used are typical of those employed in fusion operations. The NaOH and Na_2O_2 are more promising agents since dissolution of these materials would leave the actinides as hydrated oxides or hydroxides and the resulting solutions could be filtered, evaporated, and the residues heated to give soda ash. Soda ash is a glass-former; therefore, this method would not increase the final waste volume because the addition of soda ash is required anyway. Also, these materials would not add sulfate to the wash.

Heating with the Meker burner (open crucible) failed to reduce the ash weight to the extent expected, while firing would produce refractory oxides.

7.5 Conclusions

From the preliminary investigation, it may be concluded that:

(1) Recovery of >99% of the actinides in incinerator residue by simple HNO_3 leaching is not probable.

(2) Fusion offers the best chance of dissolving ash to facilitate the recovery of actinides.

(3) Fusion with basic materials would appear to offer more acceptable wastes to process.

7.6 Future Work

Although the percent of ash dissolved should give an indication of the recoverability of the actinides, the weight method is by no means conclusive. Work is under way to prepare contaminated ash to permit radiochemical analysis. Two ashes will be used: an interim ash, prepared by contaminating cold ash with plutonium nitrate and oxide and fluidizing the resulting mixture at $\sim 50^{\circ}C$; and actual contaminated ash, prepared by adding plutonium to combustible waste and burning it in a laboratory-scale FBI system. In addition to the general-trash ash being used in tests, ash produced by incineration of ion exchange resins and spent solvents will be investigated. The methods being developed using cold ash will be used for each type of ash.

The primary investigation of leaching and fusion methods is scheduled to be completed by the end of March. Promising recovery methods will be more extensively investigated from April until the end of FY 1977. FY 1978 will be spent in investigating and documenting the candidate recovery process(es). Determination of actinide losses to the off-gas system will be made concurrently with leaching and fusion experiments using contaminated ash.

7.7 Reference for Section 7

1. C. R. Cooley and R. E. Lerch, "The Acid Digestion Process for Treatment of Combustible Wastes," in Management of Plutonium-Contaminated Solid Wastes, Proceedings of the N.E.A. Seminar at Marcoule, 1974, Nuclear Energy Agency, Organization for Economic Cooperation and Development, Paris, 1974, pp. 172-85.

8. ACTINIDE RECOVERY AND RECYCLE PREPARATION FOR WASTE STREAMS

J. D. Navratil, L. L. Martella, and C. E. Plock (Rockwell International, Rocky Flats Plant)

The objective of this task is to determine the feasibility of removing actinides from secondary aqueous waste streams likely to be produced during reactor fuel fabrication and reprocessing. The waste streams are part of two flowsheets entitled "Salt Water Management" and "Acid and Waste Water Management." Evaluation of methods for the salt waste and waste-water streams and recycle preparation problems will be the major emphasis of this task.

8.1 Introduction

This is a new project at Rocky Flats; thus no prior work has been done. However, other programs which are related to this project have been under development.

Work on decreasing the plutonium concentration in liquid waste streams has been under way for the past four years at Rocky Flats. Plutonium concentrations in acidic waste streams have been decreased from 10^{-3} to 10^{-5} g/liter by application of evaporation techniques coupled with anion exchange. Development of a secondary americium process using a bidentate organophosphorous extractant has also been under investigation for the past year. These processes have been designed for use in a new $140 million plutonium recovery facility.

Complete water recycle will be utilized in a new water recovery facility at Rocky Flats. The water will be purified by reverse osmosis, which has been under development at Rocky Flats for the past five years.

8.2 Salt Waste Management

Figure 8.1 presents a conceptual flowsheet for salt waste management. Although fuel reprocessing waste streams are shown, it is envisioned that the salt wastes from a fuel fabrication plant could be treated in a similar manner. The cooling water will be sent to water purification, whereas it may be necessary to treat the tributyl phosphate (TBP) scrub by another process. An organic removal step may be needed; thus investigations of organic removal processes for waste water could apply here.

Three experimental approaches are presently planned for processing salt wastes: bidentate extraction, combined tributyl phosphate--bidentate extraction, and cation exchange. Testing of a bidentate organophosphorus solvent extraction for determining the feasibility of removing actinides from salt waste streams has been initiated. The extractant dihexyl-N,N-diethylcarbamylmethylene phosphonate is being evaluated in a batch contactor as well as on a macroporous sorbent support using an extraction chromatographic technique.

Impure (∿50%) DHDECMP was obtained from the Wateree Chemical Company, Lugoff, South Carolina. The impure DHDECMP contains an impurity which prevents efficient stripping of actinides at low acidity. This impurity was removed by passing 30 vol % DHDECMP-CCl_4 through a bed of Amberlyst®* A-26 (a macroreticular, strong-base, anion exchange resin in the hydroxide form). Americium extraction coefficients of the DHDECMP before and after impurity removal are shown in Table 8.1.

---

*Product of the Rohm and Haas Co., Philadelphia, Pa.

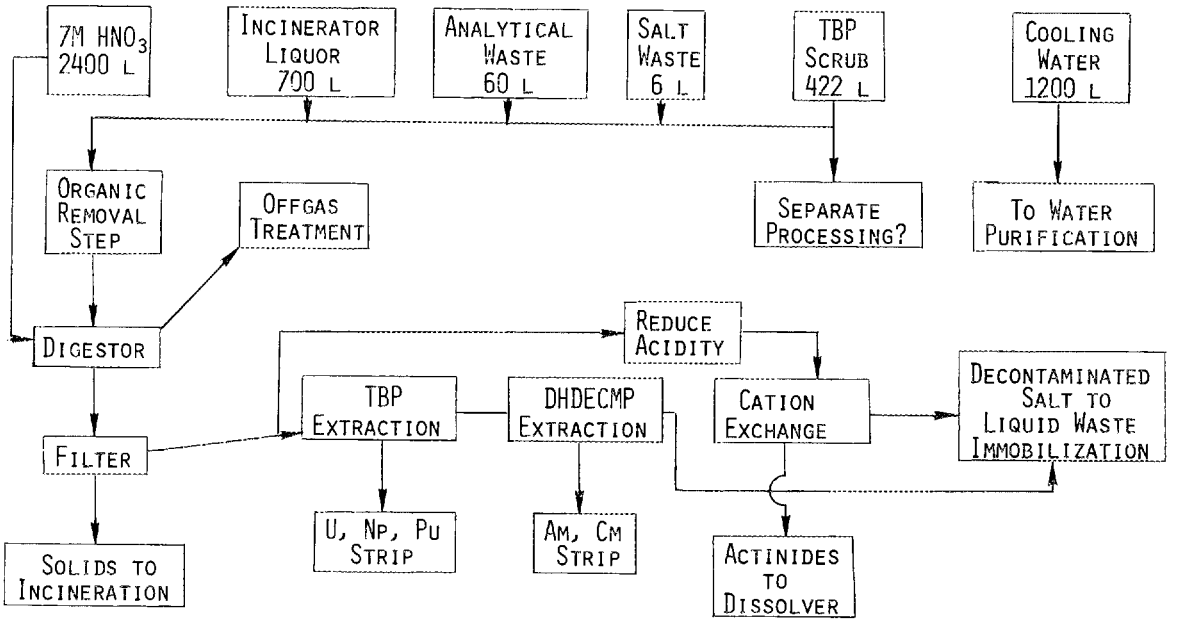

Fig. 8.1. Conceptual flowsheet for salt waste management.

Table 8.1. Americium extraction coefficients of impure DHDECMP-CCl_4 before and after resin treatment

Resin treatment?	HNO_3 (M)	Americium extraction coefficients[a] of DHDECMP (vol %)			
		30	50	70	100
Yes	0.35	0.09	0.42	1.3	3.3
Yes	7.0	1.9	15	43	53
No	0.35	125	---	---	116
No	7.0	5.5	---	---	68

[a]Estimated accuracy, ±25%.

Extraction coefficients for uranium, plutonium, and americium vs nitric acid concentration are shown in Fig. 8.2. The values for uranium at 5, 7, and 9 M HNO_3 were all $>10^3$ (and hence are off the top of the figure). The high uranium extraction coefficients at low acidity indicate that uranium stripping reagents other than water or dilute HNO_3 will be needed. However, the DHDECMP could still contain impurities causing the high uranium extraction at low activity.

8.3 Waste-Water Management

A determination of the feasibility of using reverse osmosis (RO) for water purification has been initiated. Figure 8.3 shows the conceptual flowsheet for purification of waste water containing insignificant quantities of corrosive anions and low concentrations of impurities and radioactivity. This conceptual flowsheet could also apply to any tritiated waste stream.

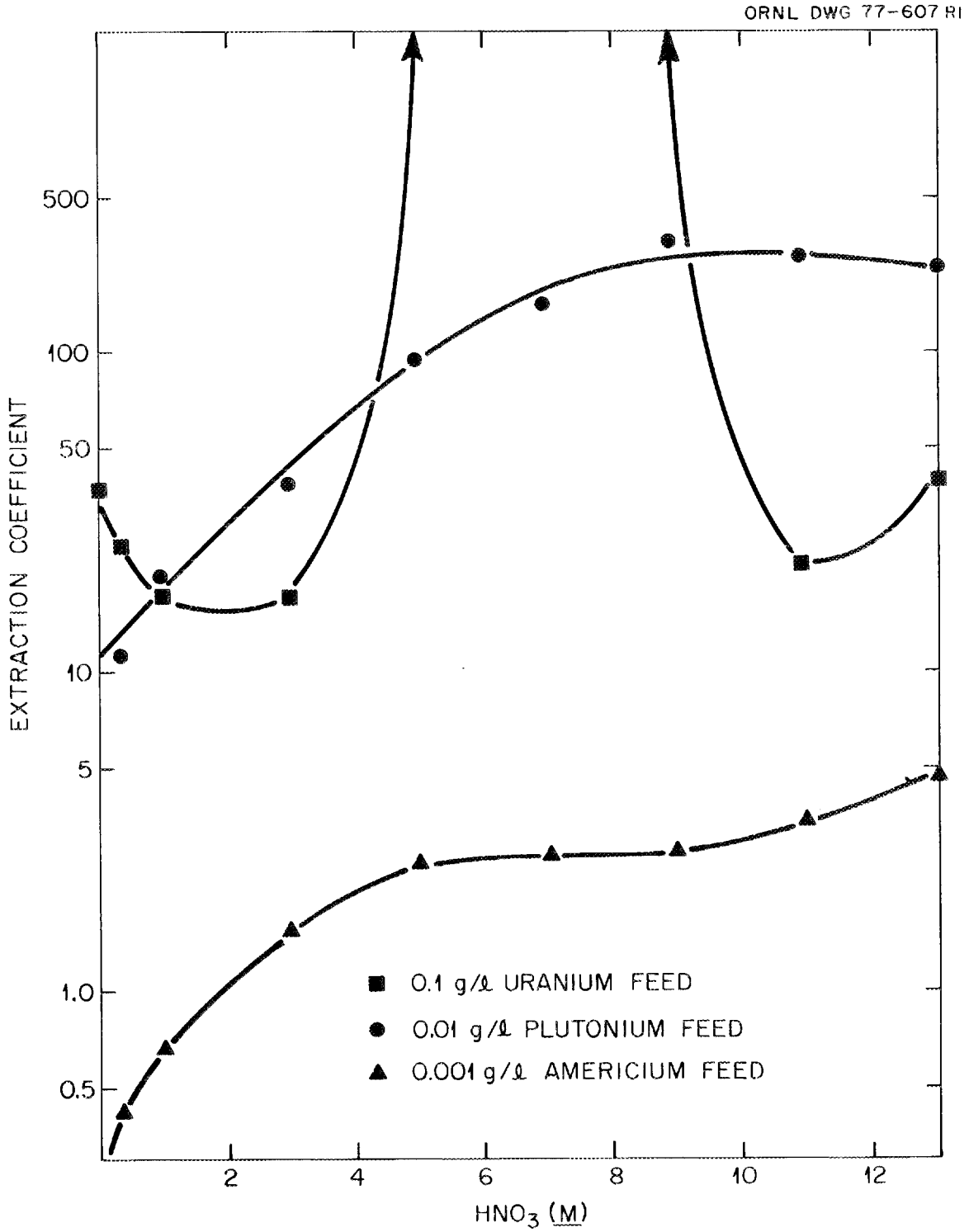

Fig. 8.2. Effect of nitric acid concentration on actinide extraction coefficients.

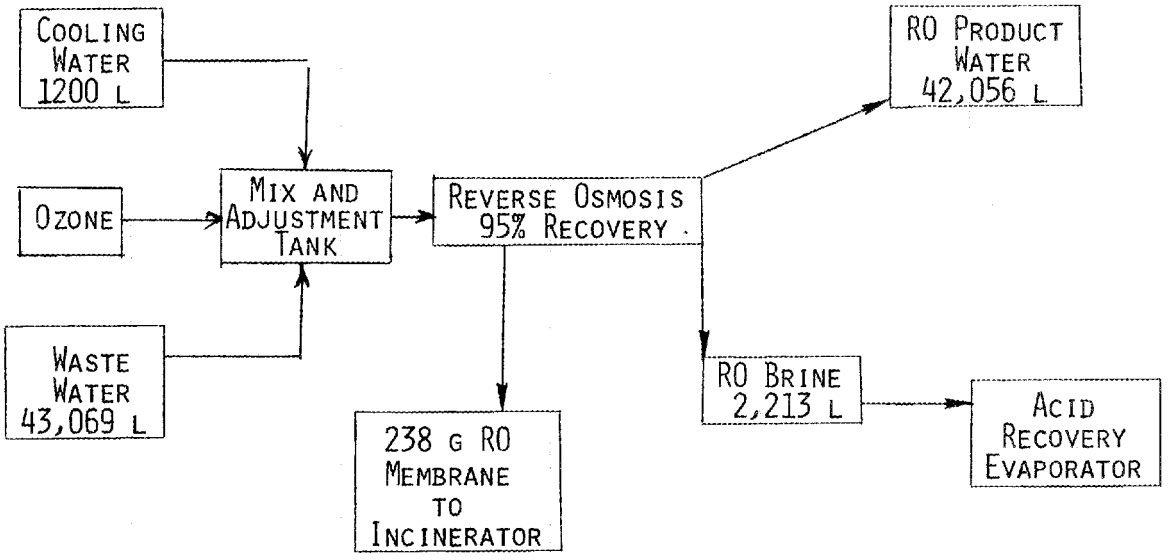

Fig. 8.3. Conceptual flowsheet for purification of waste water containing negligible quantities of anions and low concentrations of impurities and radioactivity.

The RO method is capable of reducing the volume of a waste stream by as much as 95%. The reduction of the waste stream will depend on the osmotic pressure of the impurities in the brine generated and on the composition of the impurities in the waste stream. If the concentration of the impurities is high, the osmotic pressure will be high, resulting in a decrease in the flux and desired water recovery. If the impurities in the waste stream are substances with low solubilities, such as silica and the salts of calcium, barium, and strontium, the possibility of scaling the membranes is increased. If scaling does take place, the flux will be reduced.

The advantages of RO are that it is a low-energy-consuming process, waste-water stream adjustment is minimal, and the quantity of combustible waste generated is small.

Figure 8.4 shows the conceptual flowsheet for purification of waste water containing significant quantities of anions and/or detergents. The methods planned for flowsheet testing include adsorption, RO, ultrafiltration, ion exchange, and combinations thereof. The flowsheet applies to both tritiated and nontritiated waste streams.

Ultrafiltration (UF) methods would be used mainly for the removal of detergents and would need to be coupled with an anion removal step, such as RO. Use of UF and/or RO methods would reduce the quantities of waste materials for incineration as compared with absorption--ion exchange methods.

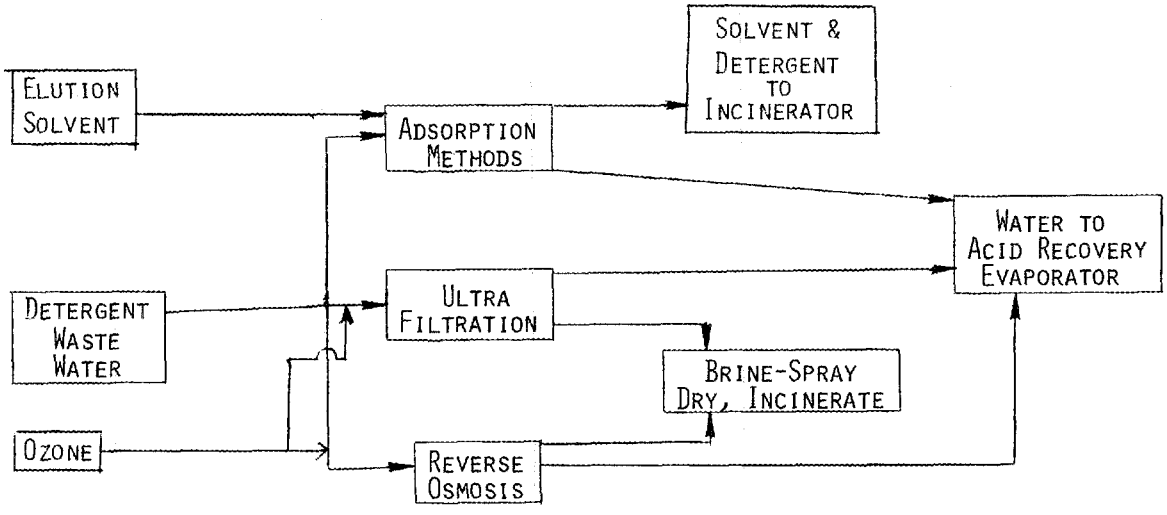

Fig. 8.4. Conceptual flowsheet for purification of waste water containing significant quantities of anions and/or detergents.

8.4 Future Work

A bidentate extraction process will be evaluated for processing salt wastes. New and recycled extractants will be tested with synthetic waste to determine actinide decontamination factors. During the investigation with synthetic waste solutions, problems of acidifying and digesting the salt wastes will be investigated.

Adsorption materials will be evaluated for removing detergents and corrosive anions from waste-water streams. Conceptual flowsheets for RO, UF, and ion exchange will also be evaluated.

9. RADIATION EFFECTS

T. E. Gangwer and M. Goldstein (Brookhaven National Laboratory)

This task examines the formation of radiation products in waste streams encountered in fuel reprocessing and refabrication plants which operate with a high degree of stream recycle. Analysis will provide methods of predicting the formation of chemical species which interfere with process operations or result in operating hazards.

During this report period, Brookhaven National Laboratory completed a review of the literature pertaining to effects of ionizing radiation on the degradation of chemical reagents used in partitioning. This review has been divided into three basic categories: (1) ion exchange materials, (2) miscellaneous, and (3) solvents.

9.1 Ion Exchange Materials

During the past 30 years, ion exchange technology has assumed increased importance in connection with the processing of solutions containing radioactive materials. The ionizing radiation produces changes in the chemical and physical properties of ion exchange materials, which generally result in a deterioration of the ion exchange capacity. The experimental conditions reported in the literature involve some type of degradation (change in exchange capacity, swelling tendency, change in selectivity of sorption, and changes in exchange kinetics) of a particular ion exchange material as a function of the type of dose (alpha, beta, or gamma).

Little attention was paid to the chemical products or the particular chemical changes in functional groups on the ion exchange materials until

May 1976, when two workers in Hanford (Building 242Z) were contaminated with americium because of an explosion. This explosion may have been caused by the reaction of highly irradiated ion exchange material in a column with 7.3 M HNO_3. The high internal dose, which is about 10^8 rads, causes severe degradation in the capacity of most commercial organic ion exchange materials. This is caused primarily by chain scission, cross-linking or destruction of the functional groups, and secondary reactions with radicals and intermediates, generally generated from the miscellaneous materials contained in the solvents. These degradation processes generally include gas evolution, changes in degree of saturation, oxidation as well as molecular rearrangement, and changes in porosity and color.

Certain inorganic ion exchangers have recently become of interest for the separation of radioactive materials because of their much higher resistance to radiation damage (i.e., approximately 10^{10} rads before significant degradation occurs). These inorganic ion exchangers, which include zirconium phosphate, molybdate, tungstate, zirconium and tin oxide and hydroxides, niobates, and titanates, have a high resistance to heat as well. Thus the inorganic ion exchange resins would, at first glance, appear to offer some prime advantages over the more-conventional organic ion exchange resins.

A review document on this subject is being prepared in an attempt to systematize the data available on the radiation chemistry of ion exchange material. Mechanisms of radiation chemical transformation will also be examined in the hope of predicting and preventing the formation of explosive materials. For example, it is known that, in the presence of

oxygen, peroxides may be formed by irradiation of organic ion exchange materials. Some of these peroxides could present an explosion hazard unless they are decomposed as rapidly as they are formed or are reacted with some scavenger material in the column.

In order to understand the radiation chemistry that is taking place with these complicated resin systems, one must look at the fundamental principle of radaiation chemistry and extrapolate. This is due to the lack of experimental investigation of the chemistry. Some evidence tells us that the radical formed in solution, such as ·OH, NOO·, HNOO·, etc., contributed significantly to the degradation mechanisms; thus the degradation products formed.

A sample of some of this radiation chemistry for several interesting miscellaneous compounds is given below.

9.2 Miscellaneous

9.2.1 Carboxylic acids

For carboxylic acids, the bond most susceptible to radiation cleavage is the carbon-carbon bond linking the carboxyl groups to the main chain. Hydrogen and carbon dioxide are liberated on irradiation, leaving as a principal product the saturated hydrocarbon with one carbon less than the original acid (and its corresponding dimer at sufficiently high carboxylic acid concentrations).

Radiolysis of carboxylic acids in the presence of oxygen prevents combination of carbon radicals to form products of higher molecular weight; oxidized products are formed instead. Thus, in the presence of oxygen, formation of peroxides, hydroperoxides, and aldehydes begins to occur.

The radiation chemistry of aqueous formic acid solutions has been extensively investigated and shows features which may be regarded as typical for organic compounds irradiated in aqueous solution. For this reason, a review of the radiation chemistry of this system will serve as a good foundation on which to build our understanding of the radiation chemistry of the carboxylic acids in particular and of organic molecules in general.

9.2.2 Radiation chemistry of formic acid (HCOOH)

The oxidation of formic acid in acid solution shows features which may be regarded as typical for organic compounds irradiated in aqueous solutions. In deoxygenated acid solutions, hydrogen and carbon dioxide are produced in approximately equal amounts and are independent of formic acid concentration in the range 0.001 to 0.01 M. The molecular products are dependent on pH where it is noted that carbon monoxide is also a product for the more acidic solutions. Both hydrogen atoms and hydroxyl radicals react with formic acid. Thus, for acidic aqueous solutions, the radiation-induced dissociation of water into free radical and molecular products,

$$H_2O \longrightarrow H\bullet,\ HO\bullet,\ H_2,\ H_2O_2,$$

is followed by the reactions

$$H\bullet + HCOOH \rightarrow H_2 + HOOC\bullet$$

$$HO\bullet + HCOOH \rightarrow H_2O + HOOC\bullet$$

$$2\ HOOC\bullet \rightarrow HCOOH + CO_2,$$

giving the net reaction

$$HCOOH \longrightarrow H_2 + CO_2.$$

The formate ion, $HCOO^-$, reacts 230 times faster with hydrogen atoms and 4 times faster with hydroxyl radicals than does the undissociated formic acid HCOOH. Thus, as the pH increases, the yields of H_2 and CO_2 fall off due to the competing reactions:

$$H\bullet + HCOO^- \longrightarrow H_2 + \bullet COO^-$$

$$HO\bullet + HCOO^- \longrightarrow HO^- + HOOC\bullet$$

$$2\bullet COO^- \longrightarrow {}^-OOCCOO^-$$

In the presence of oxygen, the yield of H_2 is reduced while the yield of H_2O_2 is increased considerably. The effect of oxygen is attributed to the removal of hydrogen atoms and $\bullet COOH$ radicals by the reactions

$$H\bullet + O_2 \longrightarrow HOO\bullet$$

$$\bullet COOH + O_2 \longrightarrow HOO\bullet + CO_2,$$

followed by either

$$2HOO\bullet \longrightarrow H_2O_2 + O_2$$

or

$$\bullet COOH + HOO\bullet \longrightarrow H_2O_2 + CO_2,$$

giving as the net reaction in the presence of oxygen:

$$HCOOH + O_2 \longrightarrow H_2O_2 + CO_2.$$

Increases in the formic acid concentration and/or solution acidity for those solutions result in increased oxygen consumption and H_2O_2 formation and lower $CO_2 + H_2$ yields.

When small amounts of hydrogen peroxide are present, the irradiation-induced decomposition of formic acid solutions results in dramatic changes in the product yields.

The chosen formation of CO_2 apparently proceeds through the reactions

$$\bullet COOH + H_2O_2 \longrightarrow CO_2 + \bullet OH + H_2O$$

$$\bullet COO^- + H_2O_2 \longrightarrow CO_2 + \bullet OH + OH^-,$$

giving the overall coupled oxidation-reduction reaction

$$HCOOH + H_2O_2 \longrightarrow 2H_2O + CO_2.$$

At low H_2O_2 concentrations, the chain is terminated by the reaction of $\bullet COOH$ and COO^- radicals with impurities, while at high H_2O_2 concentrations the chain-terminating steps are:

$$\bullet OH + H_2O_2 \longrightarrow H_2O + HOO\bullet$$

$$\bullet H + H_2O_2 \longrightarrow \bullet OH + H_2O.$$

Addition of inorganic ions to formic acid solutions changes the radiation-induced chain reaction mechanism. This can result in large changes in product yields. For example, formic acid reacts with ferrous ions and oxygen under irradiation, giving a $G(Fe^{3+})$ of 300. The overall reaction is:

$$HCCOH + 2\ Fe^{2+} + O_2 + 2H^+ \longrightarrow CO_2 + 2H_2O + 2Fe^{3+},$$

which means that the decomposition of formic acid has been increased by approximately a factor of 50 with respect to high-acidity solutions without ferrous ions.

9.2.3 Radiation chemistry of oxalic acid (HOOCCOOH)

Oxalic acid yields formic acid, carbon dioxide, and hydrogen when irradiated in aqueous solutions. The yields for destruction of oxalic acid are about the same for neutron (G = 5.2) or gamma-ray (G = 4.9) irradiation. In the presence of metal ions, a coupled oxidation-reduction system is formed such that the oxalic acid reacts by a chain mechanism when irradiated with X-, beta- or gamma-rays. The $G(CO_2)$ was found to increase from 4 to 7.5 as the oxalic acid concentration increased from 10^{-4} to 0.1 M. The $G(H_2)$ decreased from 1.5 to 0.5 over the same range. The yield of carbon dioxide was reported to decrease as the pH was increased from 3 to 7. A detailed study of the oxalate system was carried out for solutions over the pH range of 0.5 to 2.0. Doses employed ranged from one million to one hundred million rads for these air-free solutions. For solutions containing oxalic acid at concentrations of 0.02 N or higher, the observed product yields were $G(CO_2) = 7.8$, $G(H_2) = 0.46$, $G(CH_2O) = 0.08$, and $G(CHOCHO) = 0.004$, which corresponded to the decomposition of 4.9 molecules of oxalic acid per hundred electron volts of energy deposited [i.e., $G(^{-}H_2C_2O_4) = 4.9$]. The yields were independent of temperature and dose rate. The value for $G(^{-}H_2C_2O_4)$ decreases with increasing pH above 2, becoming constant at 1.96 over the 5 to 10 pH range. The change in yield was attributed to the change in form of the oxalate from the molecule $H_2C_2O_4$ to the ion $C_2O_4^{2-}$. For irradiation at lower doses in air-saturated solutions at pH below 2, the yields were $G(CO_2) = 5.6$, $G(H_2) = 0.46$, $G(H_2O_2) = 4.0$, and $G(^{-}H_2C_2O_4) = 2.9$.

For example, reduction of mercuric chloride by oxalic acid is a well-known chain reaction. In the presence of 5×10^{-6} M Fe^{3+}, Eler's reaction yields a $G(CO_2)$ of 180, which is independent of radiation intensity and the concentrations of reagents over a considerable range. This chain reaction is quite sensitive of impurities.

9.2.4 Radiation chemistry of glycolic acid ($HOCH_2COOH$)

Gamma irradiation of dilute (0.01 M), aqueous glycolic acid solutions yield water, hydrogen, and tartaric acid as the main products. Secondary products formed are oxalic acid, formic acid, and carbon dioxide. The yield of hydrogen gas reaches a maximum value of 4.2 between 0.01 and 0.5 M glycolic acid at pH = 1 and decreases rapidly upon further concentration increases. At pH 4.2, the yield for 0.01 M solutions is $G(H_2)$ = 2.0.

Aqueous glycolic acid solutions irradiated in the presence of oxygen give glyoxylic acid ($HCOCO_2HH$) and its degradation and oxidation products as the main species, with the formation of tartaric acid suppressed.

10. FUEL AND TARGET FABRICATION STUDIES

J. P. Drago and D. W. Tedder (Oak Ridge National Laboratory)

This task identifies primary and secondary transuranic waste streams and evaluates waste treatment processing options for fabrication plants that are operated under the actinide partitioning concept. Chemical and equipment flowsheets will be prepared for use in a detailed cost estimate of these plants.

A study was initiated to determine probable chemical flowsheets for handling the primary and secondary transuranic waste streams from an LWR mixed-oxide (MOX) fuel fabrication plant that was operated under the actinide partitioning concept. The model plant receives uranium and plutonium oxides, mechanically blends the oxides, presses the powder into pellets, and inserts the pellets into fuel rods. The plant also reprocesses and recycles scrap, and processes and packages all radioactive wastes generated on site. Volumes, activities, and quantities of MOX material on combustible and noncombustible trash and HEPA filters were obtained from ERDA-76-43. Unit operations supporting a MOX fabrication plant include: leaching of actinides from incinerator ashes, HEPA filters, and noncombustibles; dissolution of off-specification contaminated scrap; solvent extraction purification of uranium and plutonium; nitrate-to-oxide conversion; incineration of combustibles; and acid and water recycle. Incineration of combustibles is required to facilitate actinide recovery, reduce waste volumes, and produce a stable waste form acceptable for geologic isolation.

Reference conceptual flowsheets for this system supporting a MOX plant have been prepared and will be presented in a preliminary assessment of the concept to be published in the near future.

11. LMFBR TRANSMUTATION STUDIES

M. L. Williams and J. W. McAdoo (Oak Ridge National Laboratory)

The objective of this task is to examine the in-reactor aspects of long-lived nuclide transmutation in projected commercial LMFBRs. During FY 1977, this subtask will be concerned with scoping studies leading to the determination of one or two preferred transmutation modes which will be examined in detail in FY 1978.

The selected reactor configuration is based on a model of a 1200-MW(e) commercial LMFBR used in transmutation studies by Beaman,[1] with the following modifications:

1. The structural material will be stainless steel 316 with the same volume fraction as the structure in ref. 1.
2. The initial oxide core (driver) fuel will be composed of plutonium discharged from a uranium-enriched LWR (55% ^{239}Pu, 25% ^{240}Pu, 15% ^{241}Pu, 6% ^{242}Pu) and depleted uranium (0.25% ^{235}U).
3. Axial and radial blankets will initially contain depleted uranium only.

Depletion calculations have been performed on this reactor in RZ geometry by using the CITATION[2] computer code and five energy group ENDF/B-IV cross sections, and by assuming that the LMFBR reload fuel is enriched with the plutonium discharged from the reactor. These calculations lead to the following equilibrium results:

Reactor power -- 1200 MW(e); 3430 MW(t)

Average driver fuel burnup -- 110,000 MW/tonne heavy metal

Cycle length -- 270 full-power days

Capacity factor -- 0.80

Fuel management -- Refuel one-third of core plus axial blanket and one-sixth of radial blanket every 270 full-power days.

Future calculations will be based on preliminary ENDF/B-V cross sections currently available. These cross sections are being processed at the present time and should be available in January 1977.

11.1 References for Section 11

1. Cooperative Nuclear Data and Methods Development Third Quarterly Report January - March 1976, GEAP-14074-3 (April 1976).

2. T. B. Fowler and D. R. Vondy, Nuclear Core Analysis Code: CITATION, ORNL/TM-2496, Rev. 2 (July 1971).

12. THERMAL REACTOR TRANSMUTATION STUDIES

E. J. Hennelly and T. C. Gorrell (Savannah River Laboratory)

The objective of this subtask is to examine the in-reactor aspects of long-lived nuclide transmutation in thermal reactors. Uranium- and plutonium-enriched LWRs will be the principal reactor types examined, although "CANDU" and high-power-density (SRL production type) thermal reactors will also be examined. During FY 1977, this subtask will be concerned with scoping studies leading to the determination of one or two preferred thermal reactor transmutation modes which will be examined in detail in FY 1978.

Final approval was received in mid-December 1976, thus limiting progress for this period. However, as part of another program and in anticipation of approval of this program, the ORIGEN[1] fission product and depletion code was made operational on the SRL 360/195. This code will be useful in the future for intercomparison of actinide depletion calculations with other laboratories. In addition, comparison of uranium depletion and plutonium buildup calculations for PWRs was made with detailed experimental data on Yankee and H. B. Robinson fuel using GLASS (an integral transport depletion code) and 84 energy group cross sections. These studies were begun in support of LWR programs being administered by SRL. We plan to incorporate the results of these depletion and buildup studies as benchmark calculations for use by ORNL to improve the cross section input to ORIGEN. Studies will begin next quarter on benchmark GLASS depletion studies for actinide burnup in PWR lattices.

12.1 Reference for Section 12

1. M. J. Bell, ORIGEN - The ORNL Isotope Generation and Depletion Code, ORNL-4628 (May 1973).

13. FUEL CYCLE IMPACT STUDIES

A. G. Croff (Oak Ridge National Laboratory)

The objective of this task is to analyze the impacts of partitioning-transmutation which are not being considered by other subtasks. Examples of such impacts are the effects of the recycled actinide neutron activity on nuclear fuel cycle operations and determination of the recycled actinide inventories in the fuel cycle.

This task was not active during this report period because of the time required to prepare the preliminary partitioning-transmutation assessment report (ORNL/TM-5808).

14. RISK/BENEFIT ANALYSIS OF CONCEPT

(Oak Ridge National Laboratory and Battelle Northwest)

The objective of this task is to estimate the additional risks that are incurred as a result of increased handling of the long-lived nuclides, and the long-term benefits that would accrue as a result of the biologically significant, long-lived nuclide content of radioactive wastes being significantly reduced.

This task is not active during FY 1977.

15. DETAILED ECONOMIC ANALYSIS OF FABRICATION AND REPROCESSING PLANTS IN A PARTITIONING-TRANSMUTATION FUEL CYCLE

(Oak Ridge National Laboratory)

This task will provide detailed cost estimates of fuel reprocessing and refabrication plants operating with and without partitioning and transmutation. The analysis will show the economic impacts of this option on the fuel cycle.

This task was inactive during FY 1977.

16. PARTITIONING-TRANSMUTATION ANALYSIS, COORDINATION, AND EVALUATION

D. W. Tedder, J. P. Drago, A. G. Croff, and J. O. Blomeke (Oak Ridge National Laboratory)

This task coordinates all other efforts related to the program. Integrated flowsheets are developed from the experimental evaluation of subsystems within the fuel and target reprocessing and refabrication plants. Alternative flowsheets are evaluated; options are chosen for detailed analysis. Constraints are defined which facilitate the integration of the concept to all aspects of the fuel cycle.

During this report period, the emphasis was on development of reference material balance flowsheets which describe waste systems supporting a modified Purex reprocessing plant and a MOX refabrication plant. These integrated waste systems rely on acid and water recycle to minimize uncontrolled losses. Supplemental decontamination operations reduce losses to stable, immobilized waste effluents. The required waste treatment systems include additional processing of the HA raffinate from Purex, separation of the lanthanides from the transplutonium actinides, salt and solid waste decontamination, additional acid and water recycle operations, and off-gas treatment. Significant development work is required to implement this concept; the preliminary material balance flowsheets provide a basis for coordination of the experimental investigations.

The final partitioning flowsheets for detailed economic and risk analysis are expected to evolve through a series of iterations between engineering coordination and the experimental investigators. The strategy is to define specific waste streams and route the calculated

effluents to the appropriate recycle stations. This system analysis facilitates the identification of subproblems that can be examined experimentally. As the subproblems are verified or modified by experimental investigations, the various input and output streams will be redefined and the system analysis repeated. Hopefully, repeated iteration between the system analysis and the experimental evaluation of specific subproblems will lead to feasible flowsheets in a timely manner.

The reference material balance flowsheets developed during this period represent the first iteration in the analysis. Program participants reviewed this work, and comments were made during site visits. Alternative flowsheets are now being prepared, and the effects of the proposed modifications will be analyzed with respect to the overall system operations. This work will be published as part of a preliminary assessment of the concept.

INTERNAL DISTRIBUTION

1-2. Central Research Library
3. Document Reference Section
4-6. Laboratory Records
7. Laboratory Records, R.C.
8. ORNL Patent Section
9. C. W. Alexander
10. R. E. Blanco
11-22. J. O. Blomeke
23. W. D. Bond
24. R. E. Brooksbank
25. W. D. Burch
26. D. O. Campbell
27. A. G. Croff
28. J. P. Drago
29. D. E. Ferguson
30. G. F. Flanagan
31. L. M. Ferris
32. C. W. Forsberg
33. R. W. Glass
34. H. W. Godbee
35. J. R. Hightower
36. G. H. Jenks
37. F. A. Kappelmann
38. S. Katz
39. O. L. Keller
40. E. Lamb
41. R. E. Leuze
42. K. H. Lin
43. A. P. Malinauskas
44. W. C. McClain
45. L. E. McNeese
46. J. G. Moore
47. E. Newman
48. E. L. Nicholson
49. K. J. Notz
50. J. R. Parrott, Sr.
51. H. Postma
52. F. M. Scheitlin
53. C. D. Scott
54. R. R. Shoun
55. D. W. Tedder
56. L. M. Toth
57. D. B. Trauger
58. B. L. Vondra
59. B. Weaver
60. M. L. Williams
61. R. G. Wymer
62. C. D. Zerby
63. E. L. Gaden, Jr. (consultant)
64. C. H. Ice (consultant)
65. R. B. Richards (consultant)

EXTERNAL DISTRIBUTION

66-92. Technical Information Center, Oak Ridge, Tn 37830

ERDA-ORO, Oak Ridge, TN 37830
93. Research and Technical Support Division
94. J. J. Schreiber

ERDA, Washington, D. C. 20545
95. J. L. Burnett
96. W. K. Eister
97. R. W. Ramsey

U. S. Nuclear Regulatory Commission, Washington, D. C. 20555
98. C. B. Bartlett
99. W. P. Bishop

Allied Chemical Corp., P. O. Box 2204, Idaho Falls, ID 83401
100. L. D. McIsaac
101. C. M. Slansky

Atlantic Richfield Hanford Company, P. O. Box 250, Richland, WA 99352
102. H. Babad
103. W. W. Schulz

Battelle Northwest, P. O. Box 999, Richland WA 99352
104. A. M. Platt
105. K. J. Schneider
106. E. J. Wheelwright
107. H. C. Burkholder

Argonne National Laboratory, 9700 South Cass Ave., Argonne, IL 62439
108. E. P. Horwitz
109. G. W. Mason
110. M. Steindler

Hanford Engineering Development Laboratory, P. O. Box 1970, Richland, WA 99352
111. R. Lerch

Sandia Laboratories, P. O. Box 5800, Albuquerque, NM 87115
112. R. L. Schwoebel
113. D. R. Tallant

George C. Marshall Space Flight Center, Marshall Space Flight Center, AL 35812
114. R. E. Burns

Mound Laboratory, P. O. Box 32, Miamisburg, Ohio 45342
115. E. L. Lewis
116. D. F. Luthy

Rockwell International, Rocky Flats Plant, P. O. Box 464, Golden, CO 80401
117. F. J. Miner
118. J. D. Navratil
119. G. H. Thompson

E. I. du Pont de Nemours and Company, Savannah River Laboratory, Aiken, South Carolina 29801
120. T. C. Gorrell
121. E. J. Hennelly

Brookhaven National Laboratory, Upton, New York 11973
122. T. E. Gangwer

Los Alamos Scientific Laboratory, P. O. Box 1663, Los Alamos, NM 37544
123. W. J. Maraman

Atomic Energy Research Establishment, Harwell, Didcot, Oxon., OX11 ORA, England
124. N. J. Keen
125. G. N. Kelly

Centre d'études nucléaires de Fontenay-aux-Roses, B.P. No. 6, Fontenay-aux-Roses, France
126. Y. Sousselier

OECD-Nuclear Energy Agency, 38, Boulevard Suchet, F-75016 Paris, France
127. M. Takahashi

International Atomic Energy Agency, P. O. Box 590, A-1011 Vienna, Austria
128. J. R. Grover

Institut für Heisse Chemie Kernforschungszentrum, Postfach 3640, 75 Karlsruhe, Germany
129. H. O. Haug

Lab. Teoria e Calcolo Reottori, C.N.E.N. - C.S.N. Casaccia, CP 2400 I-00100 Rome, Italy
130. L. Tondinelli

Commission of the European Communities, CCR Euratom, I-21200 Ispra, Italy
131. F. Girardi

Nuclear Research Institute, 25066 Rez, Czechoslovakia
132. L. Neumann

Chalmers University of Technology, Dept. of Nuclear Chemistry S-402 20 Göteborg, Sweden
133. J. O. Liljenzin

☆ U.S. GOVERNMENT PRINTING OFFICE: 1977-748-189/78